Concerning the nature of high-T_c superconductivity: Survey of experimental properties and implications for interlayer coupling

D. R. Harshman and A. P. Mills, Jr.
AT&T Bell Laboratories, Murray Hill, New Jersey 07974
(Received 16 October 1991)

An increasing body of data suggests the existence of a unique set of criteria characterizing "ideal" high-T_c superconductivity. Common to those materials exhibiting these high-T_c characteristics, i.e., the layered cuprates and certain layered organic superconductors, is the reduced dimensionality of the superfluid density. In cases where the carriers are confined to two dimensions, the parameters specifying the superconducting state would include the two-dimensional carrier density n_{2D}, the interlayer spacing d, the two-dimensional effective mass m_{ab}^*, the two-dimensional Fermi energy E_F^{2D}, and the average dielectric constant ϵ. To determine these parameters, we tabulate the relevant known properties on a variety of two- and three-dimensional superconductors. While partially limited by the quality of existing data, we nevertheless find that the data representative of the phase-pure high-T_c-like layered compounds of simple geometry, with stoichiometry optimized for minimum disorder effects and highest T_c, exhibit clean-limit correlations of the form $n_{2D}d^2=1$, $m_{ab}^* \propto \epsilon/d$, $k_B T_c \propto 1/\epsilon d \propto E_F^{2D}$, and $H_{1/2} \propto H_0$. Here, H_0 is a characteristic field related to the upper critical field and $H_{1/2}$ is the characteristic field at which the specific-heat jump at T_c is reduced to half its zero-field value. The observed correlations may be understood in terms of a simple interlayer Coulomb-coupling hypothesis.

INTRODUCTION

Soon after the discovery of high-temperature superconductivity,[1] its unconventional properties led Anderson[2] to suggest that phonons could not be responsible for the attractive force binding the Cooper pairs.[3] Unlike their conventional counterparts, the high-T_c cuprate superconductors are normally characterized by carriers that are confined to two dimensions; a resistivity above the superconducting transition temperature, T_c, that is proportional to the temperature, T; a curious absence of coherence factor effects that ordinarily would lead to the Hebel-Slichter[4] anomaly in the T_1 nuclear relaxation rate below T_c; a reduced isotope effect on T_c; an unusually short clean-limit Pippard coherence length; and transition temperatures that seem too high to be accounted for by phonon coupling. On the other hand, the existence of quasiparticle pairs of charge $2e$,[5] and the temperature dependence of the energy gap reflect a BCS-like character.[6] Furthermore, muon spin rotation (μ^+SR) and subsequent magnetization measurements of the pairing state indicate zero orbital angular momentum, and thus s-wave pairing.[7] While one normally associates high-T_c superconductivity with the layered cuprates, we shall see that certain layered organic superconductors, which do not have particularly high transition temperatures, also exhibit high-T_c-like characteristics.

Recent advances in the fabrication and characterization of the high-T_c cuprates are beginning to suggest the existence of a unique set of criteria characterizing "ideal" high-T_c superconductivity. Although there is no consensus on what is required for high-T_c superconductivity, experiment appears to restrict the range of possibilities. The observed anisotropies in the resistivity and magnetic penetration depth, the occurrence of a metal-insulator transition at carrier densities corresponding to the single-plane sheet resistance[8] expected for a two-dimensional (2D) transition, as well as the strong field dependence of the specific-heat jump at T_c, indicate that the carriers are confined to two dimensions. Although there are arguments to the contrary,[9,10] the observed tendency towards a vanishing isotope effect also appears to be inconsistent with phonon mediation, while the s-wave character of the gap function makes it difficult to consider most spin-coupling mechanisms. Furthermore, while there are conventional ways of accounting for the lack of coherence effects,[11] their absence may indicate that the Cooper pairing is not occurring within a single plane. The interference terms in the electron-phonon scattering could vanish if the pairing were to occur between quasiparticles in neighboring planes, and if the paired states are essentially degenerate with respect to the parity of the two-particle wave functions in the direction perpendicular to the planes, which is equivalent to a negligible hopping rate for particles between planes. The suppression of isotope and coherence effects, as well as the existence of s-wave pairing, could thus be understood within the context of a Coulomb-mediated mechanism coupling carriers in neighboring conducting sheets.

In this paper, we examine the experimental properties of the high-T_c superconductors assuming BCS theory as the appropriate framework. With the aim of exposing new systematic trends, and bearing in mind the possible importance of interlayer Coulomb coupling, we will search for correlations among various measurements. The parameters we wish to investigate would then include the interplanar spacing d, as well as the properties relating to a single sheet, such as the 2D carrier density,

n_{2D}, the 2D effective mass, m_{ab}^*, the 2D Fermi energy, E_F^{2D}, and the sheet resistance of a single conducting plane just above the transition temperature, $R(T_c)$. As one might expect, there has been considerable experimental effort already spent in searching for meaningful relationships connecting T_c with other electronic properties of the high-T_c cuprates and other materials. Unfortunately, these studies often neglected the effects of disorder or did not explicitly take into account the 2D character of the problem. Our approach will be to consider the least ambiguous experimental data, described in the following sections.

Although the superconducting properties of the high-T_c cuprates have been extensively investigated using a variety of techniques, only a few have yielded unambiguous information that might be useful in understanding the superconducting mechanism. Of particular relevance to our investigation are the two-dimensional carrier density and effective mass, which for conventional phonon-mediated superconductivity are derived from normal-state transport and Hall-effect measurements. Complications arising from sample inhomogeneity, a relatively unattainable upper critical field, temperature-dependent Hall coefficients, and other complex normal-state phenomena have made a determination of these quantities for the high-T_c superconductors through conventional means somewhat difficult. However, three of the more reliable measured quantities, the magnetic penetration depth (derived from transverse field μ^+SR), the specific-heat jump, $\Delta C/T_c$, and the interatomic spacings, are sufficient, assuming a single parabolic band, to determine n_{2D} and m_{ab}^*. In some cases, where specific-heat or penetration depth measurements are unavailable, we may obtain from titration measurements[12] an estimate of n_{2D} for certain simple structures.

In the following sections, we describe how the relevant parameters are derived, and tabulate the known associated properties for a variety of superconductors, including the layered cuprates. We then discuss the effects of disorder on the measurements, search for correlations within the context of a simple interlayer Coulomb-coupling model, and present our conclusions.

EXPERIMENTAL SYSTEMATICS

In order to write explicit relations between the experimentally determined quantities, we assume a single parabolic band and the validity of the effective-mass approximation for the relevant carriers. For type-II superconductors, the zero-temperature limit of the effective magnetic penetration depth, $\lambda_{\rm eff}(T)$, is generally given by[13]

$$\lambda_{\rm eff}(0)\approx\left[1+\frac{\xi_0}{l}\right]^{1/2}\lambda_L(0)=\left[1+\frac{\xi_0}{l}\right]^{1/2}\left[\frac{m^*/m_e}{4\pi n_{3D}r_e}\right]^{1/2}, \tag{1}$$

where ξ_0 is the coherence distance, l the mean free path, $r_e=e^2/m_ec^2$ ($=2.82\times10^{-5}$ Å) the classical electron radius, n_{3D} the superfluid (single-particle) carrier density, m^* the average component of the effective-mass tensor in the plane perpendicular to the applied field, and m_e the free-electron mass. Notice that if ξ_0 is comparable to l, the measured value, $\lambda_{\rm eff}(0)$, can become significantly larger than the London value, $\lambda_L(0)$. As will be discussed later, l may be estimated from the resistivity.

In the case of weak coupling, the Sommerfeld constant γ is directly related to the specific-heat jump at T_c via the equation, $1.43\gamma=\Delta C/T_c$. For a free-electron gas in three dimensions, the Sommerfeld constant is

$$\gamma^{3D}=\left[\frac{\pi}{3}\right]^{2/3}k_B^2\frac{m^*}{\hbar^2}(n_{3D})^{1/3}. \tag{2}$$

For a stack of identical two-dimensional conducting planes with average spacing δ,[14]

$$\gamma^{2D}=\frac{\pi}{3}k_B^2\frac{m_{ab}^*}{\hbar^2}\frac{1}{\delta}, \tag{3}$$

where m_{ab}^* is now the average 2D effective mass in the plane of the conducting sheets, normally the ab basal plane. For the high-T_c materials, for which the crystal structure is normally comprised of a series of CuO_2 planes, Eq. (3) is clearly more appropriate, and the relevant penetration depth is the London (clean-limit) basal-plane value, $\lambda_{ab}(0)$. Solving Eq. (3) for m_{ab}^*, we have

$$\frac{m_{ab}^*}{m_e}=7.102\frac{\Delta C}{T_c}\frac{\delta}{V_m}, \tag{4}$$

where $\Delta C/T_c$ is in units of mJ K^{-2}/(mole formula unit), δ is in Å, and V_m is the volume per formula unit in Å^3. Note that assuming strong coupling would reduce the extracted m_{ab}^* value. Also, when written in terms of the penetration depth, the two-dimensional Fermi energy is independent of $n_{2D}=n_{3D}\delta$ and is given by

$$E_F^{2D}=\pi\hbar^2\frac{n_{2D}}{m_{ab}^*}=\frac{\hbar^2c^2}{4e^2}\frac{\delta}{\lambda_{ab}^2(0)},\qquad \frac{E_F^{2D}}{k_B}=7.85\times10^8\frac{\delta}{\lambda_{ab}^2(0)}, \tag{5}$$

with δ and $\lambda_{ab}(0)$ given in Å and E_F^{2D}/k_B in K. Solving Eq. (5) for n_{2D} we then have

$$n_{2D}=3.60\times10^{-4}\frac{m_{ab}^*}{m_e}\frac{E_F^{2D}}{k_B}, \tag{6}$$

with n_{2D} in units of 10^{14} cm^{-2}. Thus, by knowing δ, $\lambda_{ab}(0)$, and $\Delta C/T_c$ from experiments, it is possible to calculate n_{2D}, m_{ab}^*, and E_F^{2D}.

For three-dimensional materials, we use Eqs. (1) and (2) to find the effective mass, thus

$$\frac{m^*}{m_e}=\lambda_L^{1/2}(0)r_e^{1/4}\left[\frac{\Delta C\hbar^2}{k_B^2T_cm_e}\right]^{3/4}\left[\frac{36}{1.43^3\pi}\right]^{1/4}=0.604\lambda_L^{1/2}(0)\left[\frac{\Delta C}{V_mT_c}\right]^{3/4}, \tag{4a}$$

the Fermi energy,

$$E_F^{3D}=\frac{\hbar^2}{2m^*}(3\pi^2 n_{3D})^{2/3},$$
$$\frac{E_F^{3D}}{k_B}=1.000\times 10^8 \lambda_L^{-3/2}(0)\left[\frac{\Delta C}{V_m T_c}\right]^{-1/4}, \quad (5a)$$

and the 3D carrier density,

$$n_{3D}=\frac{m^*}{m_e}\frac{1}{4\pi\lambda_L^2(0)r_e}$$
$$=1.705\times 10^6 \lambda_L^{-3/2}(0)\left[\frac{\Delta C}{V_m T_c}\right]^{3/4}, \quad (6a)$$

with n_{3D} given in units of 10^{21} cm^{-3}.

MEASUREMENTS

We have assembled in Tables I and II the relevant parameters on a variety of high-T_c cuprates. For comparison, we include representative materials from the organic, intercalated-chalcogenide, bismuthate, electron-doped cuprate, Chevrel phase, intercalated-graphite, alkali-metal fulleride (e.g., A_3C_{60}), uranium-based heavy fermion, and $A15$ superconducting families. The references for the Tables are included in the Appendix. Only a few of the compounds have been sufficiently researched to provide unambiguous information regarding all of the electronic parameters listed in Table I. We comment on the various entries in the tables as follows.

Table I: Electronic parameters

(1) Transition temperature, T_c and ΔT_c. The superconducting transition temperatures are well known for most of the compounds, as are the transition widths ΔT_c (10%–90%). Unless otherwise stated, the T_c's quoted are the maximum known values for the structure and stoichiometry. In some cases ΔT_c increases as T_c falls upon substitution, signifying increasing inhomogeneous disorder.

(2) Isotope effect, α. The dependence of T_c on the isotopic mass (i.e., $T_c \propto M^{-\alpha}$, where M is the isotopic mass) is generally regarded as an important measure of the electron-phonon interaction. While the original BCS theory predicted (for weak coupling) $\alpha=0.5$,[6] the inclusion of Coulomb interactions can significantly alter this expectation. Where it is known, the oxygen isotope ($^{16}O\rightarrow{}^{18}O$) exponent α is small or consistent with zero for the cuprates of optimum compositions, but has a value of 0.42, typical of a nearly ideal phonon-mediated BCS superconductor, for $Ba_{1-x}K_xBiO_3$.[15] Recent studies[16] of K_3C_{60} give $\alpha=0.30\pm0.06$, also suggesting phonon-mediated BCS superconductivity. One of the more significant features of the isotope effect in the high-T_c cuprates is the strong dependence on stoichiometry. This is most easily seen in the $La_{2-x}Sr_2CuO_4$ system,[17] where $\alpha=0.4\pm0.05$ for $x=0.1$, while reducing to 0.140 ± 0.008 for $x\geq 0.15$. Equally interesting is the $(Y_{1-x}Pr_x)Ba_2Cu_3O_7$ system, where α changes monotonically from near zero for $x=0$ to 0.34 ± 0.03 for $x=0.4$.[18] These data are plotted against T_c in Fig. 1.

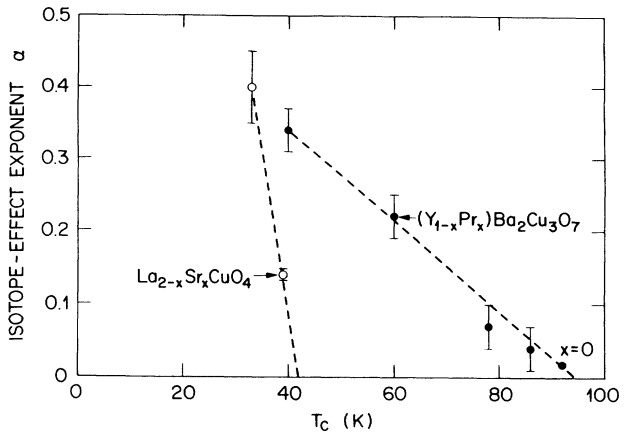

FIG. 1. The exponent, α (oxygen isotope effect), vs the superconducting transition temperature, T_c. The solid and open symbols correspond to $(Y_{1-x}Pr_x)Ba_2Cu_3O_7$ and $La_{2-x}Sr_xCuO_x$. Data taken from Refs. 18 and 17, respectively.

(3) Normal state resistivity, $\rho(T>T_c)$. One imperative for considering the temperature dependence of the normal-state resistivity is its connection to the mean free path l, which, if comparable to the coherence length ξ_0, may affect the measured value of the penetration depth according to Eq. (1). The normal-state resistivity for most of the high-T_c cuprates tends to exhibit a linear temperature dependence of the form, $\rho(T>T_c)=\rho(0)+\beta T$. The interesting feature of the temperature coefficient $\beta=d\rho/dT$, is that for any given material it tends toward an intrinsic value, and decreases with disorder. In many cases, as the superconducting properties of a material improves, the residual resistivity $\rho(0)$ decreases and eventually vanishes with optimization. There are numerous observations of depressed T_c associated with an enhanced $\rho(0)$ in nonoptimum samples.[19] This increase in disorder effects is not necessarily associated with increasing crystalline disorder. Indeed, there is increasing experimental evidence pointing to intrinsic crystalline disorder which is not observed to effect the optimized superconducting state. Figure 2 shows $\rho(0)$ versus

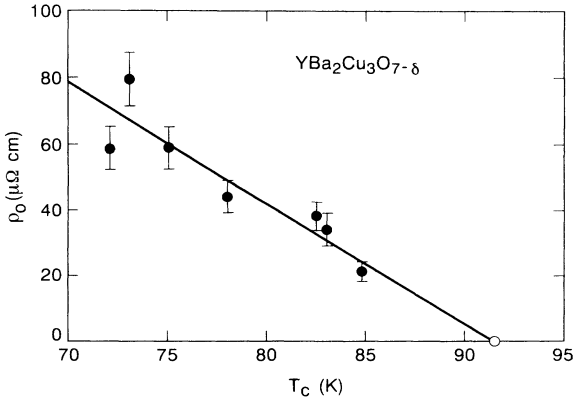

FIG. 2. The residual basal-plane resistivity, $\rho(0)$, for a set of thin-film $YBa_2Cu_3O_{7-\delta}$ samples plotted vs T_c. Data taken from Laderman *et al.*, in Ref. 19.

TABLE I. Measured electronic parameters for the various materials. The times denoted by an asterisk are discussed in more detail in the Appendix.

No.	Compound	T_c (K)	ΔT_c (K)	α	$\rho(0)$; $\rho(T_c)$ ($\mu\Omega$cm)	Coherence Effects	$\Delta C/T_c$ (mJ/mol K^2)	$H_{1/2}$ (Tesla)	$\lambda(0)$ (Å)	$H_{c2_\parallel}(0)$ (Tesla)
1.	$La_{1.9}Sr_{0.1}CuO_4$	33	6.5	0.4±0.05	$\propto T+c$	No	3.85*	x	3200±160	x
	$La_{1.875}Sr_{0.125}CuO_4$	36	4.5	x	$\propto T+c$	x	5.3*	x	2700±135	x
	$La_{1.85}Sr_{0.15}CuO_4$	39	2	0.140±0.008	0 ; 33±6	No	17.5±2	x	2185±100	45±10
	$La_{1.775}Sr_{0.225}CuO_4$	29	7.5	0.1±0.03	$\propto T+c$	x	5.3*	x	x	x
	$La_{1.725}Sr_{0.275}CuO_4$	22	10	0.12±0.05	$\propto T+c$	x	1.75*	x	x	x
2.	$La_{1.6}Sr_{0.4}CaCu_2O_6$	60	~10	x	$\propto T+c$	x	x	x	x	x
3.	$YBa_2Cu_3O_{6.67}$	60	1	x	x ; 63±8	No	11±4	x	2550±125	87
4.	$YBa_2Cu_3O_7$	92	1	0.018±0.004	0 ; 40±5	No	50±10	3±1	1415±30	140±30
	$HoBa_2Cu_3O_7$	92	1	x	x ; x	x	55±10	x	x	x
	$PrBa_2Cu_3O_7$	0	–	–	–	–	–	–	–	–
	$(Y_{0.95}Pr_{0.05})Ba_2Cu_3O_7$	90	1.8	x	50 ; 100	x	x	x	1500±75	x
	$(Y_{0.9}Pr_{0.1})Ba_2Cu_3O_7$	86	2.2	0.04±0.03	50 ; 100	x	x	x	1730±85	x
	$(Y_{0.8}Pr_{0.2})Ba_2Cu_3O_7$	78	3.2	0.07±0.03	100 ; 140	x	x	x	1980±100	x
	$(Y_{0.7}Pr_{0.3})Ba_2Cu_3O_7$	60	7.5	0.22±0.03	250 ; 280	x	x	x	2150±100	x
	$(Y_{0.6}Pr_{0.4})Ba_2Cu_3O_7$	40	13.2	0.34±0.03	300 ; 335	x	x	x	2900±150	x
	$YBa_2(Cu_{0.99}Fe_{0.01})_3O_7$	91	1.3	x	x ; x	x	46	x	x	x
	$YBa_2(Cu_{0.975}Fe_{0.025})_3O_7$	85	3	x	x ; x	x	24	x	x	x
	$YBa_2(Cu_{0.95}Fe_{0.05})_3O_7$	75	5	x	x ;	x	<10	x	x	x
	$YBa_2(Cu_{0.99}Zn_{0.01})_3O_7$	78	1	x	$\propto T$	x	32±4	x	x	x
	$YBa_2(Cu_{0.975}Zn_{0.025})_3O_7$	62	1	x	150;200	x	13	x	x	x
	$YBa_2(Cu_{0.95}Zn_{0.05})_3O_7$	36	1.5	x	240;300	x	7.2	x	x	x
5.	$YBa_2Cu_4O_8$ (ambient press.)	80	2	x	$\propto T+c$*	No	16±2	x	1980±100	x
	$YBa_2Cu_4O_8$ (10 GPa)	107	x	x	x	x	x	x	x	x
	$HoBa_2Cu_4O_8$ (ambient press.)	80	5	x	100 ; 400	x	~5*	x	1610±80	x
6.	$Bi_2Sr_2CuO_{6+\delta}$	8.5	1	x	100 ; 109	x	x	x	x	x
	$Bi_2(Sr_{1.6}La_{0.4})CuO_{6+\delta}$	23.5	x	x	320 ; 360	x	x	x	x	x
	$(Bi,Pb)_2(Sr_{1.75}La_{0.25})CuO_6$	24	x	x	x ; x	x	x	x	x	x
	$(Bi,Pb)_2(Sr_{1.8}Pr_{0.2})CuO_6$	15	x	x	x ; x	x	x	x	x	x
	$(Bi,Pb)_2(Sr_{1.75}Nd_{0.25})CuO_6$	17	x	x	x ; x	x	x	x	x	x
7.	$Bi_2Sr_2CaCu_2O_8$ (no-anneal)	89	1	x	0 ; 38±2	No	32±10*	x	2500±500*	107
	$Bi_2Sr_2CaCu_2O_{8+\delta}$ (O_2 annealed)	75	1	0.037±0.004	$\propto T$	No	x	x	x	x
8.	$Bi_2Sr_2Ca_2Cu_3O_{10}$	107	~10	x	0 ; <60*	x	18±5	x	x	x
	$(Bi_{1.6}Pb_{0.4})Sr_2Ca_2Cu_3O_{10}$	107	1	0.026±0.002	0 ; x	No	32±8	x	2525±300	184
9.	$Tl_2Ba_2CuO_6$	85	x	x	40 ; 100*	No	x	x	1700±100*	x
10.	$Tl_2Ba_2CaCu_2O_8$	99	x	x	0±20 ; 300±80	No	35±10*	x	2210±100	99
11.	$Tl_2Ca_2Ba_2Cu_3O_{10}$	125	x	x	20 ; 83	No	24±8	x	1960±100	75
12.	$(Tl_{0.7}Cd_{0.3})BaLaCuO_5$	48	x	x	x ; x	x	x	x	x	x
13.	$(Tl_{0.5}Pb_{0.5})Sr_2CaCu_2O_7$	80	x	x	x ; x	x	13±2*	x	1816±90*	x
	$(Tl_{0.5}Pb_{0.5})Sr_2(Ca_{0.8}Y_{0.2})Cu_2O_7$	107	x	x	0 ; 250	x	22±2*	x	x	x
14.	$(Tl_{0.5}Pb_{0.5})Sr_2Ca_2Cu_3O_9$	122	x	x	$\propto T+c$	x	x	x	1580±80	x
15.	$Pb_2(Y_{1-x}Ca_x)Sr_2Cu_3O_8$	80	x	x	50 ; 250	No	x	x	x	x
16.	$(Nd_{2-x}Ce_x)CuO_4$	24	2	≤0.05	250 ; 250*	No	~1.7	x	x	x
17.	κ–[BEDT–TTF]$_2$Cu[NCS]$_2$	10.5	x	x	10±150*; 330±50	No	48±5	0.2±0.1	7500±1000	~10*
18.	$[TMTSF]_2ClO_4$	1.2	0.1	x	nonlinear	No	15±2	0.02±0.005	12000±2000	0.10±0.02*
19.	A_3C_{60} (K_3C_{60},...,Rb_2CsC_{60})	31.3	1	0.30±0.06*	~const.*	No	x	x	<5100*	~30*
20	KC_8	0.55	0.05	x	x	x	x ; x	x	x	x
21.	$TaS_2(Py)_{1/2}$	3.4	x	x	const.	x	36±8	x	2350±250	0.214±0.025
22.	$Ba_{0.6}K_{0.4}BiO_3$	32	8	0.42±0.05	2000 ; 2000	x	2.2±0.4	~6	3450±200	17
23.	$BaPb_{0.75}Bi_{0.25}O_3$	11	x	0.22±0.03	340 ; 340	x	2.3±0.3	x	10000±500	7±1.5
24.	$PbMo_6S_8$ (Chevrel)	12	0.5	0.27±0.04*	50 ; 90	x	10±2	9±1	2700±400	55
25.	UPt_3	0.53	x	x	0.2 ; 0.5	No*	300±50	~0.6	6960±37	2.1
26.	Nb_3Sn	17.9	0.2	0.08±0.02*	8.8 ; 8.8	x	25±3	8±1	640±30*	37

TABLE II. Measured structural parameters and assumed values for the average plane spacings δ and interlayer spacings *d*. Other possible values of δ and *d*, which are discussed briefly in the text, are given in the square brackets.

No.	Compound	a (Å)	b (Å)	c (Å)	δ (Å)	d (Å)	Space Group	V_m (Å^3/f.u.)	Density (g cm^{-3})
1.	$La_{1.9}Sr_{0.1}CuO_4$	3.7839(8)	3.7839(8)	13.211(4)	6.61	6.61	I4/mmm	94.6	7.02
	$La_{1.875}Sr_{0.125}CuO_4$	3.7784(8)	3.7784(8)	13.216(4)	6.61	6.61	I4/mmm	94.4	7.02
	$La_{1.85}Sr_{0.15}CuO_4$	3.7793(1)	3.7793(1)	13.2260(3)	6.62	6.62	I4/mmm	95.0	7.00
	$La_{1.775}Sr_{0.225}CuO_4$	3.7708(8)	3.7708(8)	13.247(3)	6.62	6.62	I4/mmm	94.2	6.94
	$La_{1.725}Sr_{0.275}CuO_4$	3.7666(8)	3.7666(8)	13.225(3)	6.61	6.61	I4/mmm	93.8	6.92
2.	$La_{1.6}Sr_{0.4}CaCu_2O_6$	3.8208(1)	3.8208(1)	19.5993(7)	4.9	3.39	I4/mmm	143.1	6.04
3.	$YBa_2Cu_3O_{6.67}$	3.831(2)	3.889(2)	11.736(6)	5.87	11.74 [5.9?]	Pmmm	174.9	6.28
4.	$YBa_2Cu_3O_7$	3.8198(1)	3.8849(1)	11.6762(3)	5.84	3.36	Pmmm	173.3	6.39
	$HoBa_2Cu_3O_7$	3.846(1)	3.881(1)	11.640(2)	5.82	3.31	Pmmm	173.7	7.09
	$PrBa_2Cu_3O_7$	3.905(2)	3.905(2)	11.660(10)	5.83	3.47	Pmmm	177.8	6.71
	$(Y_{0.95}Pr_{0.05})Ba_2Cu_3O_7$	x	x	x	x	≈3.36	Pmmm	x	x
	$(Y_{0.9}Pr_{0.1})Ba_2Cu_3O_7$	x	x	x	x	≈3.36	Pmmm	x	x
	$(Y_{0.8}Pr_{0.2})Ba_2Cu_3O_7$	x	x	x	x	≈3.36	Pmmm	x	x
	$(Y_{0.7}Pr_{0.3})Ba_2Cu_3O_7$	x	x	x	x	≈3.36	Pmmm	x	x
	$(Y_{0.6}Pr_{0.4})Ba_2Cu_3O_7$	x	x	x	x	≈3.36	Pmmm	x	x
	$YBa_2(Cu_{0.99}Fe_{0.01})_3O_7$	x	x	x	x	≈3.36	Pmmm	x	x
	$YBa_2(Cu_{0.975}Fe_{0.025})_3O_7$	x	x	x	x	≈3.36	Pmmm	x	x
	$YBa_2(Cu_{0.95}Fe_{0.05})_3O_7$	x	x	x	x	≈3.36	Pmmm	x	x
	$YBa_2(Cu_{0.99}Zn_{0.01})_3O_7$	x	x	x	x	≈3.36	Pmmm	x	x
	$YBa_2(Cu_{0.975}Zn_{0.025})_3O_7$	3.820(2)	3.890(2)	11.673(6)	5.84	≈3.36	Pmmm	173.5	6.39
	$YBa_2(Cu_{0.95}Zn_{0.05})_3O_7$	3.820(2)	3.885(2)	11.671(6)	5.84	≈3.36	Pmmm	173.2	6.39
5.	$YBa_2Cu_4O_8$ (ambient press.)	3.86(1)	3.86(1)	27.24(6)	6.81	3.38	Ammm	202.9	6.10
	$YBa_2Cu_4O_8$ (10 GPa)	3.79	3.79	26.75	6.69	3.32	Ammm	192.1	6.45
	$HoBa_2Cu_4O_8$ (ambient press.)	3.855(1)	3.874(1)	27.295(11)	6.82	~3.3	Ammm	203.8	6.70
6.	$Bi_2Sr_2CuO_{6\pm\delta}$	5.361(2)	5.370(1)	24.369(6)	12.15	12.15	Cmmm	175.4	7.13
	$Bi_2(Sr_{1.6}La_{0.4})CuO_{6+\delta}$	5.370(5)	5.400(5)	24.50(2)	12.25	12.25	Cmmm	177.6	7.23
	$(Bi,Pb)_2(Sr_{1.75}La_{0.25})CuO_6$	5.282(5)	5.410(5)	24.62(1)	12.31	12.31	Cmmm	175.9	7.23
	$(Bi,Pb)_2(Sr_{1.8}Pr_{0.2})CuO_6$	5.264(5)	5.412(5)	24.27(1)	12.14	12.14	Cmmm	172.9	7.33
	$(Bi,Pb)_2(Sr_{1.75}Nd_{0.25})CuO_6$	5.249(5)	5.419(5)	24.24(1)	12.12	12.12	Cmmm	172.4	7.39
7.	$Bi_2Sr_2CaCu_2O_8$ (no-anneal)	5.413(2)	5.411(2)	30.91(1)	7.73	3.35	Fmmm	226.4	6.52
	$Bi_2Sr_2CaCu_2O_{8+\delta}$ (O_2 annealed)	5.408(2)	5.413(2)	30.81(1)	7.70	3.35	Fmmm	225.5	6.54
8.	$Bi_2Sr_2Ca_2Cu_3O_{10}$	5.39	5.39	37.1	9.27	6.70 [3.35?]	Fmmm	269.5	6.26
	$(Bi_{1.6}Pb_{0.4})Sr_2Ca_2Cu_3O_{10}$	5.413(3)	5.413(3)	37.100(12)	9.27	6.70 [3.35?]	Fmmm	271.8	6.31
9.	$Tl_2Ba_2CuO_6$	3.866(1)	3.866(1)	23.239(6)	11.60 [5.8?]	11.60 [5.8?]	I4/mmm	173.7	8.06
10.	$Tl_2Ba_2CaCu_2O_8$	3.8550(6)	3.8550(6)	29.318(4)	7.33	3.2	I4/mmm	217.8	7.46
11.	$Tl_2Ca_2Ba_2Cu_3O_{10}$	3.8503(6)	3.8503(6)	35.88(3)	8.97	6.42 [3.21?]	I4/mmm	266.6	6.96
12	$(Tl_{0.7}Cd_{0.3})BaLaCuO_5$	3.844(2)	3.844(2)	9.16(1)	9.16 [4.6?]	9.16 [4.6?]	P4/mmm	135.4	7.32
13.	$(Tl_{0.5}Pb_{0.5})Sr_2CaCu_2O_7$	3.8023(3)	3.8023(3)	12.107(1)	6.05	3.24	P4/mmm	174.0	6.30
	$(Tl_{0.5}Pb_{0.5})Sr_2(Ca_{0.8}Y_{0.2})Cu_2O_7$	3.8075(3)	3.8075(3)	12.014(2)	6.05	3.24	P4/mmm	174.2	6.30
14.	$(Tl_{0.5}Pb_{0.5})Sr_2Ca_2Cu_3O_9$	3.8206(2)	3.8206(2)	15.294(1)	7.65	6.46 [3.23?]	P4/mmm	220.9	5.98
15.	$Pb_2(Y_{1-x}Ca_x)Sr_2Cu_3O_8$	5.3933(2)	5.4311(2)	15.7334(6)	7.87	3.45	Cmmm	230.4	7.20
16.	$(Nd_{2-x}Ce_x)CuO_4$	3.9469(2)	3.9469(2)	12.0776(5)	6.04	6.04	I4/mmm	188.2	6.72
17.	κ-[BEDT-TTF]$_2$Cu[NCS]$_2$	16.248	8.440	13.124	15.24	15.24	$P2_1$	844.0	1.87
18.	$[TMTSF]_2ClO_4$	7.266(1)	7.678(1)	13.275(2)	13.275	13.275	$P\bar{1}$	694.3	2.38
19.	A_3C_{60} (K_3C_{60},...,Rb_2CsC_{60})	14.436(2)	14.436(2)	14.436(2)	(14.44)	(14.44)	$Fm\bar{3}m$	752.1	2.11
20.	KC_8	4.961	8.592	23.76	5.94	5.94	Fdd2	126.6	1.77
21.	$TaS_2(Py)_{1/2}$	3.326	3.326	12.02	12.02	12.02	$P\bar{3}m1$	133.0	3.63
22.	$Ba_{0.6}K_{0.4}BiO_3$	4.287(6)	4.287(6)	4.287(6)	(4.29)	(4.29)	$Pm\bar{3}m$	79.0	7.47
23.	$BaPb_{0.75}Bi_{0.25}O_3$	6.0496(1)	6.0696(1)	8.6210(2)	(8.62)	(8.62)	I4/mcm	79.2	8.24
24.	$PbMo_6S_8$ (Chevrel)	6.5759(9)	6.5383(9)	6.4948(8)	(6.49)	(6.49)	$R\bar{3}/P\bar{1}$	279.2	6.18
25.	UPt_3	5.754	5.754	4.890	(4.89)	(4.89)	$P6_3/mmc$	81.0	16.88
26.	Nb_3Sn	5.289(2)	5.289(2)	5.289(2)	(5.29)	(5.29)	$Pm\bar{3}m$	74.0	8.92

APPENDIX TO TABLES I AND II

1. $La_{2-x}Sr_xCuO_4$	
Structure	R. J. Cava *et al.* Phys. Rev. B **35**, 6716 (1987).
α	L. C. Bourne *et al.* Solid State Commun. **67**, 707 (1988); For off-stoichiometric materials see M. K. Crawford *et al.*, Phys. Rev. B **41**, 282 (1990); Physica C **162-164**, 755 (1989).
$\rho(0);\rho(T_c)$	B. Batlogg, in *High Temperature Superconductivity,* edited by K. Bedell *et al.* (Addison-Wesley, New York, 1990), p. 37; J. M. Tarascon *et al.*, Science **235**, 1373 (1987).
Coherence effects	Y. Kitaoka *et al.*, J. Magn. Magn. Mater. **90&91**, 619 (1990); Y. Kitaoka *et al.*, Physica B **165&166**, 1309 (1990); T. Kobayashi *et al.*, *ibid.* **165&166**, 1299 (1990).
$\Delta C/T_c$	G. Hilscher *et al.*, Z. Phys. B **72**, 461 (1988); A. Amato *et al.* Physica B **165&166**, 1337 (1990); Relative numbers for the nonoptimal materials are taken from J. W. Loram and K. A. Mirza, in *Electronic Properties of High-T_c Superconductors and Related Materials,* edited by H. Kuzmany, M. Mehring, and J. Fink (Springer-Verlag, Berlin, 1990), p. 92.
$H_{1/2}$	*x*
$\lambda_{ab}(0)$	G. Aeppli *et al.*, Phys. Rev. B **35**, 7129 (1987), measured $La_{1.85}Sr_{0.15}CuO_4$; D. R. Harshman *et al.* (unpublished), give results for various stoichiometries.
H_{c2}	S. Uchida *et al*, Jpn. J. Appl. Phys. **26**, L443 (1987); J. M. Tarascon *et al.*, Science **235**, 1373 (1987).
2. $La_{1.6}Sr_{0.4}CaCu_2O_6$	
Structure	R. J. Cava *et al.*, Nature **345**, 602 (1990); Physica C **172**, 138 (1990).
α	*x*
$\rho(0);\rho(T_c)$	R. J. Cava *et al.*, Nature **345**, 602 (1990).
Coherence effects	*x*
$\Delta C/T_c$	*x*
$H_{1/2}$	*x*
$\lambda_{ab}(0)$	*x*
H_{c2}	*x*
3. $YBa_2Cu_3O_{6.67}$	
Structure	R. J. Cava *et al.*, *Nature* **329**, 423 (1987); Phys. Rev. B **36**, 5719 (1987); Physica C **165**, 419 (1990).
α	*x*
$\rho(0);\rho(T_c)$	R. J. Cava *et al.*, *Nature* **329**, 423 (1987); Phys. Rev. B **36**, 5719 (1987); Physica C **165**, 419 (1990).
Coherence effects	W. W. Warren *et al.*, Phys. Rev. Lett. **62**, 1193 (1989).
$\Delta C/T_c$	W. Wühl *et al.*, in *Proceedings of the M^2S-HTSC III Conference,* Kanazawa, Japan, 1991 [Physica C **185-189**, 755 (1991)].
$H_{1/2}$	*x*
$\lambda_{ab}(0)$	D. R. Harshman *et al.*, Phys. Rev. B **39**, 851 (1989); W. C. Lee and D. M. Ginsberg, *ibid.* **44**, 2815 (1991).
H_{c2}	K. G. Vandervoort *et al.*, Phys. Rev. B **43**, 13042 (1991).
4. $YBa_2Cu_3O_7$	
Structure	F. Beech *et al.*, Phys. Rev. B **35**, 8778 (1987); R. J. Cava *et al.*, Nature **329**, 423 (1987); Phys. Rev. B **36**, 5719 (1987); Physica C **165**, 419 (1990).
α	$\alpha=0.0\pm0.2$—B. Batlogg *et al.*, Phys. Rev. Lett. **59**, 912 (1987); $\alpha=0.017\pm0.006$—E. L. Benitez *et al.*, Phys. Rev. B **38**, 5025 (1988); $\alpha=0.019\pm0.004$—S. Hoen *et al.*, Phys. Rev. B **39**, 2269 (1989). $\alpha=-0.006\pm0.015$ [Cu isotope effect]—L. Quan *et al.*, Solid State Commun. **65**, 869 (1988).
$\rho(0);\rho(T_c)$	K. Semba *et al.*, Phys. Rev. Lett. **67**, 769 (1991).
Coherence effects	P. C. Hammel *et al.*, Phys. Rev. Lett. **63**, 1992 (1989).
$\Delta C/T_c$	A. Junod *et al.*, Physica C **159**, 215 (1989); E. Bonjour *et al.*, Physica B **165&166**, 1343 (1990).
$H_{1/2}$	See, e.g., E. Bonjour *et al.*, Physica B **165&166**, 1343 (1990); S. E. Inderhees *et al.*, Phys. Rev. Lett. **60**, 1178 (1988); M. B. Salamon *et al.*, Phys. Rev. B **38**, 885 (1988); V. G. Zarifis and D. H. Douglass, Physica C **170**, 46 (1990).

APPENDIX TO TABLES I AND II (*Continued*).

$\lambda_{ab}(0)$	D. R. Harshman *et al.*, Phys. Rev. B **39**, 851 (1989).
H_{c2}	K. Semba *et al.*, Phys. Rev. Lett. **67**, 769 (1991).
$HoBa_2Cu_3O_7$	
Structure	Y. Le Page *et al.*, Phys. Rev. B **36**, 3617 (1987); H. Asano *et al.*, Jpn. J. Appl. Phys. **26**, L1341 (1987).
α	*x*
$\rho(0);\rho(T_c)$	B. Batlogg, in *High Temperature Superconductivity,* edited by K. Bedell *et al.* (Addison-Wesley, New York, 1990), p. 37.
Coherence effects	*x*
$\Delta C/T_c$	C.-S. Jee *et al.*, in *Proceedings of the Drexel International Conference on High Temperature Superconductivity,* edited by S. M. Bose and S. D. Tyagi (World Scientific, Singapore, 1988), p. 133.
$H_{1/2}$	*x*
$\lambda_{ab}(0)$	*x*
H_{c2}	*x*
$PrBa_2Cu_3O_7$	
Structure	Y. Le Page *et al.*, Phys. Rev. B **36**, 3617 (1987).
α	—
$\rho(0);\rho(T_c)$	B. Batlogg, in *High Temperature Superconductivity,* edited by K. Bedell *et al.* (Addison-Wesley, New York 1990), p. 37.
Coherence effects	—
$\Delta C/T_c$	—
$H_{1/2}$	—
$\lambda_{ab}(0)$	—
H_{c2}	—
$(Y_{1-x}Pr_x)Ba_2Cu_3O_7$	
Structure	*x*
α	J. P. Franck *et al.*, Physica B **169**, 697 (1991); J. C. Phillips, Phys. Rev. B **43**, 6257 (1991).
$\rho(0);\rho(T_c)$	A. P. Goncalves *et al.*, Phys. Rev. B **37**, 7476 (1988).
Coherence effects	*x*
$\Delta C/T_c$	*x*
$H_{1/2}$	*x*
$\lambda_{ab}(0)$	C. L. Seaman *et al.*, Phys. Rev. B **42**, 6801 (1990).
H_{c2}	*x*
$YBa_2(Cu_{1-x}Fe_x)_3O_7$	
Structure	*x*
α	*x*
$\rho(0);\rho(T_c)$	*x*
Coherence effects	*x*
$\Delta C/T_c$	C. Meingast *et al.*, Physica C **173**, 309 (1991).
$H_{1/2}$	*x*
$\lambda_{ab}(0)$	W. J. Kossler *et al.*, Hyperfine Interact. **63**, 253 (1990); These authors show that the *s*-wave character of $\lambda_{ab}(T)$ is lost with increasing *x*.
H_{c2}	*x*
$YBa_2(Cu_{1-x}Zn_x)_3O_7$	
Structure	M. Affronte *et al.*, Solid State Commun. **70**, 951 (1989).
α	*x*
$\rho(0);\rho(T_c)$	M. Affronte *et al.*, Solid State Commun. **70**, 951 (1989).
Coherence effects	*x*
$\Delta C/T_c$	C. Meingast *et al.*, Physica C **173**, 309 (1991); J. W. Loram and K. A. Mirza, in *Electronic Properties of High-T_c Superconductors and Related Materials,* edited by H. Kuzmany, M. Mehring, and J. Fink (Springer-Verlag, Berlin, 1990), p. 92.

APPENDIX TO TABLES I AND II (*Continued*).

$\lambda_{ab}(0)$	W. J. Kossler *et al.*, Hyperfine Interact. **63**, 81 (1990), show that the *s*-wave character of $\lambda_{ab}(T)$ is lost with increasing x.
H_{c2}	x
5. $YBa_2Cu_4O_8$	
Structure	Ambient Pressure—P. Marsh *et al.*, Nature **334**, 141 (1988); 10 GPa—R. J. Wijngaarden *et al.* (unpublished), report a 25% reduction in V_m at this elevated pressure, concomitant with a peak in T_c at 107 K.
α	x
$\rho(0);\rho(T_c)$	S. Martin *et al.*, Phys. Rev. B **39**, 9611 (1989), show a negative $\rho(0)=-22$ $\mu\Omega$ cm, indicating that the material is possibly overdoped.
Coherence effects	x
$\Delta C/T_c$	A. Junod *et al.* (unpublished); A. Junod *et al.*, Physica B **165&168**, 1335 (1990).
$H_{1/2}$	x
$\lambda_{ab}(0)$	A. Schilling *et al.*, Physica C **168**, 272 (1990).
H_{c2}	x
$HoBa_2Cu_3O_8$	
Structure	R. J. Cava *et al.*, Physica C **159**, 372 (1989).
α	x
$\rho(0);\rho(T_c)$	A. Bernasconi *et al.*, Physica C **166**, 393 (1990).
Coherence effects	x
$\Delta C/T_c$	A. Bernasconi *et al.*, Physica C **166**, 393 (1990), quote a 9% Meissner fraction for their sample, and suggest that extrapolation to a full Meissner fraction would give $\Delta C/T_c \approx 58\text{mJ/mol K}^2$.
$H_{1/2}$	x
$\lambda_{ab}(0)$	A. Schilling *et al.* (unpublished); A. Schilling *et al.*, Z. Phys. B **82**, 9 (1991).
H_{c2}	x
6. $Bi_2Sr_2CuO_{6\pm\delta}$	
Structure	C. C. Torardi *et al.*, Phys. Rev. B **38**, 225 (1988); R. M. Fleming *et al.*, Physica C **173**, 37 (1991); J. M. Tarascon *et al.*, Phys. Rev. B **38**, 8885 (1988).
α	x
$\rho(0);\rho(T_c)$	S. Martin *et al.*, Phys. Rev. B **41**, 846 (1990).
Coherence effects	x
$\Delta C/T_c$	x
$H_{1/2}$	x
$\lambda_{ab}(0)$	x
H_{c2}	x
$Bi_2(Sr_{1-x}La,Pr_x)CuO_{6+\delta}$	
Structure	B. C. Sales and B. C. Chakoumakos, Phys. Rev. B **43**, 12 994 (1991).
α	x
$\rho(0);\rho(T_c)$	x
Coherence effects	x
$\Delta C/T_c$	We arrive at our values for n_{3D} and n_{2D} from titration measurements: $n_h=0.2$—B. C. Sales and B. C. Chakoumakos, Phys. Rev. B **43**, 12 994 (1991); $n_h=0.3$—W. A. Groen *et al.*, Physica C **165**, 305 (1990); $n_h=0.12$—A. Maeda *et al.*, Phys. Rev. B **41**, 6418 (1990).
$H_{1/2}$	x
$\lambda_{ab}(0)$	We arrive at our values for n_{3D} and n_{2D} from titration measurements: $n_h=0.2$—B. C. Sales and B. C. Chakoumakos, Phys. Rev. B **43**, 12 994 (1991); $n_h=0.3$—W. A. Groen *et al.*, Physica C **165**, 305 (1990); $n_h=0.12$—A. Maeda *et al.*, Phys. Rev. B **41**, 6418 (1990).
H_{c2}	x
$(Bi,Pb)_2(Sr_{1-x}M_x)CuO_6$ (M=La,Pr,Nd)	
Structure	V. Manivannan *et al.*, Mat. Res. Bull. **26**, 349 (1991).
α	x

APPENDIX TO TABLES I AND II (*Continued*).

$\rho(0);\rho(T_c)$	x
Coherence Effects	x
$\Delta C/T_c$	We arrive at our values for n_{3D} and n_{2D} from titration measurements: V. Manivannan *et al.*, Mat. Res. Bull. **26**, 349 (1991).
$H_{1/2}$	x
$\lambda_{ab}(0)$	We arrive at our values for n_{3D} and n_{2D} from titration measurements: V. Manivannan *et al.*, Mat. Res. Bull. **26**, 349 (1991).
H_{c2}	x
7. $Bi_2Sr_2CaCu_2O_{8+\delta}$	
Structure	D. B. Mitzi *et al.*, Phys. Rev. B **41**, 6564 (1990); J. M. Tarascon *et al.*, *ibid.* **38**, 8885 (1988).
α	H. Katayama-Yoshida *et al.*, Physica C **156**, 481 (1988).
$\rho(0);\rho(T_c)$	S. A. Sunshine *et al.*, Phys. Rev. B **38**, 893 (1988); B. Batlogg, in *High Temperature Superconductivity,* edited by K. Bedell *et al.* (Addison-Wesley, New York, 1990), p. 37; B. Batlogg *et al.*, Physica C **153-155**, 1062 (1988).
Coherence effects	Y. Kitaoka *et al.*, J. Magn. Magn. Mater. **90&91**, 619 (1990).
$\Delta C/T_c$	$\delta=0$—A. M. Bandyopadhyay *et al.*, Physica C **165**, 29 (1990); D. Wohlleben *et al.*, in *International Conference on Superconductivity,* Bangalore, India, 1990, edited by S. K. Joshi, C. N. R. Rao, and S. V. Subramanyam (World Scientific, Singapore, 1990), p. 194, observe strong fluctuation effects; O.-M. Ness *et al.*, Supercond. Sci. Tech. **4**, S388 (1991), also observe strong fluctuation effects.
$H_{1/2}$	x
$\lambda_{ab}(0)$	$\delta=0$—D. R. Harshman *et al.*, Phy. Rev. Lett. **67**, 3152 (1991); D. R. Harshman *et al.* (unpublished), present measurements on single-crystal samples, corrected for flux-motion and longitudinal disordering of the flux lines; A. Schilling *et al.*, Z. Phys. B **82**, 9 (1990), data taken on polycrystalline sample, ignoring flux motion and longitudinal disorder.
H_{c2}	$\delta=0$—J. N. Li *et al.*, Appl. Phys. A **47**, 209 (1988).
8. $Bi_2Sr_2Ca_2Cu_3O_{10}$	
Structure	J. M. Tarascon *et al.*, Phys. Rev. B **38**, 8885 (1988).
α	x
$\rho(0);\rho(T_c)$	K. Ogawa *et al.*, in *Advances in Superconductivity,* edited by T. Ishiguro and K. Kajimura (Springer-Verlag, Tokyo, 1990), p. 27. These measurements are conducted on granular *c*-axis oriented films.
Coherence effects	x
$\Delta C/T_c$	W. Schnelle *et al.*, Physica C **161**, 123 (1989).
$H_{1/2}$	x
$\lambda_{ab}(0)$	x
H_{c2}	x
$(Bi_{1.6}Pb_{0.4})Sr_2Ca_2Cu_3O_{10}$	
Structure	A. Maeda *et al.*, Jpn. J. Appl. Phys. **28**, L576 (1989); S. Kambe *et al.*, in *Advances in Superconductivity II,* edited by T. Ishiguro and K. Kajimura (Springer-Verlag, Tokyo, 1990), p. 215.
α	H. Katayama-Yoshida *et al.*, Physica C **156**, 481 (1988).
$\rho(0);\rho(T_c)$	F. Shi *et al.*, Phys. Rev. B **41**, 6541 (1990).
Coherence effects	Y. Kitaoka *et al.*, J. Magn. Magn. Mater. **90&91**, 619 (1990).
$\Delta C/T_c$	R. A. Fisher *et al.*, Physica C **162-164**, 502 (1989); R. Jin *et al.*, *ibid.* **156**, 255 (1989), report 49.5 mJ/mol K^2, but the data show significant fluctuation effects.
$H_{1/2}$	x
$\lambda_{ab}(0)$	A. Schilling *et al.*, Z. Phys. B **82**, 9 (1990).
H_{c2}	F. Shi *et al.*, Phys. Rev. B **41**, 6541 (1990).
9. $Tl_2Ba_2CuO_{6\pm\delta}$	
Structure	C. C. Torardi *et al.*, Phys. Rev. B **38**, 225, (1988); J. B. Parise *et al.*, Physica C **159**, 239 (1989).
α	x

APPENDIX TO TABLES I AND II (*Continued*).

$\rho(0);\rho(T_c)$	Y. Shimakawa *et al.*, Physica C **157**, 279 (1989); Y. Shimakawa *et al.*, Phys. Rev. B **42**, 10 165 (1990); A. Maignan *et al.*, Physica C **170**, 350 (1990), hydrogen annealing, i.e., oxygen depletion raises T_c to 92 K.
Coherence effects	F. Hentsch *et al.*, Physica C **165**, 485 (1990); Y. Kitaoka *et al.*, J. Magn. Magn. Mater. **90&91**, 619 (1990).
$\Delta C/T_c$	x
$H_{1/2}$	x
$\lambda_{ab}(0)$	M. Mehring *et al.*, Z. Phys. B 77, 355 (1989), present a rather nice NMR measurement on an oriented powder sample with $T_c \approx 85$ K.
H_{c2}	x
10. $Tl_2Ba_2CaCu_2O_8$	
Structure	J. D. Fitz Gerald *et al.*, Phys. Rev. Lett. **60**, 2797 (1988).
α	x
$\rho(0);\rho(T_c)$	$\rho(0)$—C. C. Torardi *et al.*, Science **240**, 631 (1988). $\rho(T_c)$—H. M. Duan *et al.*, Phys. Rev. B **43**, 12 925 (1991).
Coherence effects	F. Hentsch *et al.*, Physica C **165**, 485 (1990).
$\Delta C/T_c$	A. Junod *et al.*, Physica C **159**, 215 (1989). Note: $\rho(T)$ is not $\propto T$ above T_c for the sample used in the specific-heat measurements, suggesting that the $\Delta C/T_c$ measured by Junod *et al.*, may be a lower limit.
$H_{1/2}$	x
$\lambda_{ab}(0)$	A. Schilling *et al.*, Z. Phys. B **82**, 9 (1991).
H_{c2}	J. H. Kang *et al.*, Appl. Phys. Lett. **53**, 2560 (1988).
H_{c2}	x
11. $Tl_2Ca_2Ba_2Cu_3O_{10}$	
Structure	C. C. Torardi *et al.*, Science **240**, 631 (1988).
α	x
$\rho(0);\rho(T_c)$	B. Batlogg, in *High Temperature Superconductivity*, edited by K. Bedell *et al.* (Addison-Wesley, New York, 1990), p. 37; M. Hong *et al.*, *Proceedings of 16th International Conference on Metallurgical Coatings*, San Diego, CA, in "Thin Solid Films," (1989); C. C. Torardi *et al.*, Science **240**, 631 (1988).
Coherence effects	F. Hentsch *et al.*, Physica C **165**, 485 (1990).
$\Delta C/T_c$	A. Junod *et al.*, Physica C **159**, 215 (1989). Note; $\rho(T > T_c)$ is $\propto T$ for the sample used in the specific-heat measurements; A. K. Bandyopadhyay *et al.*, Physica C **165**, 29 (1990), measure 56.5 mJ/mol K^2, but the resistivity is nonlinear and the T_c is suppressed by 10 K.
$H_{1/2}$	x
$\lambda_{ab}(0)$	A. Schilling *et al.*, Z. Phys. B **82**, 9 (1991).
H_{c2}	O. Laborde *et al.*, Physica C **162&164**, 1619 (1989).
12. $(Tl_{0.7}Cd_{0.3})BaLaCuO_5$	
Structure	M. A. Subramanian and A. K. Gangull, Mat. Res. Bull. **26**, 91 (1991).
α	x
$\rho(0);\rho(T_c)$	x
$\Delta C/T_c$	x
$H_{1/2}$	x
$\lambda_{ab}(0)$	x
H_{c2}	x
13. $(Tl_{0.5}Pb_{0.5})Sr_2(Ca_{1-x}Y_x)Cu_2O_7$	
Structure	M. A. Subramanian *et al.*, Science **242**, 249 (1988); J. B. Parise *et al.*, Physica C **159**, 245 (1989); M. R. Presland and J. L. Tallon, *ibid.* **177**, 1 (1991).
α	x
$\rho(0);\rho(T_c)$	M. A. Subramanian *et al.*, Science **242**, 249 (1988); M. R. Presland and J. L. Tallon, Physica C **177**, 1 (1991). According to M. R. Presland *et al.*, *ibid.* **176**, 95 (1991), T_c, peaks at 107 K for $x = 0.2$.
Coherence effects	x

APPENDIX TO TABLES I AND II (*Continued*).

$\delta C/T_c$	J. W. Loram and K. A. Mirza, in *Electronic Properties of High-T_c Superconductors and Related Materials,* edited by H. Kuzmany, M. Mehring, and J. Fink (Springer-Verlag, Berlin, 1990), p. 92. $\Delta C/T_c = 13\pm2$ and 22 ± 2 mJ/mol K^2, for $x=0$ and 0.2, respectively.
$H_{1/2}$	x
$\lambda_{ab}(0)$	Y. J. Uemura *et al.*, Phys. Rev. Lett. **62**, 2317 (1989). Unfortunately, data were taken only for $x=0$.
H_{c2}	x
14. $(Tl_{0.5}Pb_{0.5})Sr_2Ca_2Cu_3O_9$	
Structure	M. A. Subramanian *et al.*, Science **242**, 249 (1988).
α	x
$\rho(0);\rho(T_c)$	M. A. Subramanian *et al.*, Science **242**, 249 (1988).
Coherence effects	x
$\Delta C/T_c$	x
$H_{1/2}$	x
$\lambda_{ab}(0)$	Y. J. Uemura *et al.*, Phys. Rev. Lett. **62**, 2317 (1989).
H_{c2}	x
15. $Pb_2(Y_{1-x}Ca_x)Sr_2Cu_3O_8$	
Structure	R. J. Cava *et al.*, Physica C **157**, 272 (1989).
α	x
$\rho(0);\rho(T_c)$	J. S. Xue *et al.*, Physica C **166**, 29 (1990).
Coherence effects	T. Kohara *et al.*, Physica B **165&166**, 1307 (1990).
$\Delta C/T_c$	x
$H_{1/2}$	x
$\lambda_{ab}(0)$	x
H_{c2}	x
16. $(Nd_{2-x}Ce_x)CuO_4$	
Structure	F. Izumi *et al.*, Physica C **158**, 433 (1989).
α	B. Batlogg *et al.*, in Proceedings of the M^2s HTSC III Conference, Kanazawa, Japan, 1991 [Physica C **185-189**, 1385 (1991)].
$\rho(0);\rho(T_c)$	Resistivities for a $(Sm_{1.85}Ce_{0.15})CuO_{4-y}$ single crystal; J. L. Peng *et al.*, Physica C **177**, 79 (1991), show $\rho \approx a+bT^2$.
Coherence effects	K.-i. Kumagai *et al.*, Physica B **165&166**, 1297 (1990).
$\Delta C/T_c$	M. Sera *et al.*, Solid State Commun. **72**, 749 (1989).
$H_{1/2}$	x
$\lambda_{ab}(0)$	x
H_{c2}	x
17. κ-[BEDT-TTF]$_2$Cu[NCS]$_2$	
Structure	H. Urayama *et al.*, Chem. Lett. p. 55 (1988); G. Saito *et al.*, Synth. Met. **27**, A331 (1988).
α	x
$\rho(0);\rho(T_c)$	-150;420 $\mu\Omega$ cm—K. Murata *et al.*, Synth. Met. **27**, A341 (1988); x;370 $\mu\Omega$ cm—H. Veith *et al.*, *ibid.* **27**, A361 (1988); 170;400 $\mu\Omega$ cm—A. Ugawa *et al.*, *ibid.* **27**, A445 (1988); x;280±50 (deuterated)—K. Oshima *et al.*, J. Phys. Soc. Jpn. **57**, 730 (1988); x;200—S. Gärtner *et al.*, Solid State Commun. **65**, 1531 (1988): we note that Figs. 1(a) and 1(b) disagree; we use the value from Fig. 1(a). The average of these is 10±150;330±50.
Coherence effects	T. Takahashi *et al.*, Synth. Met. **27**, A319 (1988); D. Schweitzer *et al.*, *ibid.* **27**, A465 (1988). D. R. Harshman *et al.* (unpublished) show that the peak in $1/T_1$ at ~ 5 K may be attributed to the flux-lattice transition observed in μ^+SR.
$\Delta C/T_c$	J. E. Graebner *et al.*, Phys. Rev. B **41**, 4808 (1990); $\gamma(0)$—R. G. Goodrich and J.-c. Xu, Physica B **165&166**, 889 (1990).
$H_{1/2}$	J. E. Graebner *et al.*, Phys. Rev. B **41**, 4808 (1990).

APPENDIX TO TABLES I AND II (*Continued*).

$\lambda_{bc}(0)$	D. R. Harshman *et al.*, Phys. Rev. Lett. **64**, 1293 (1990), show an effective value of $\lambda_{bc}^{\text{eff}}(0)\approx 9800$ Å for $H_{\text{ext}}=0.3$ T. However, since H_{c2} is likely to be $\lesssim 10$ T (for carriers in the *bc* plane), there is a significant correction due to the field-dependence of $\langle(\Delta B)^2\rangle$ (see Ref. 45). Taking into account finite-*l* corrections and the associated errors, we arrive at a zero-field, clean-limit value of $\lambda_{bc}(0)=7500\pm 1000$ Å.
H_{c2}	K. Murata *et al.*, Synth. Met. **27**, A341 (1988), show a nonlinear dependence in dH_{c2}/dT, which turns up towards 10 T below about 2 K.
18. $[TMTSF]_2ClO_4$	
Structure	G. Rindorf *et al.*, Acta. Crystalogr. B **38**, 2805 (1982); K. Bechgaard *et al.*, Phys. Rev. Lett. **46**, 852 (1981). Although this material consists of chainlike structural units, the observation of quantum Hall plateaus would seem to indicate that the electronic structure is two dimensional. See, e.g., S. T. Hannahs *et al.* in *Organic Superconductivity*, edited by W. A. Little (Plenum, New York, 1990), p. 133.
α	*x*
$\rho(0);\rho(T_c)$	K. Bechgaard *et al.*, Phys. Rev. Lett. **46**, 852 (1981), show $\rho(T>T_c)$ to be nonlinear.
Coherence effects	M. Takigawa *et al.*, J. Phys. Soc. Jpn. **56**, 873 (1987); D. Jerome *et al.*, Phys. Scr. **27**, T130 (1989).
$\Delta C/T_c$	P. Garoche *et al.*, Phys. Rev. Lett. **49**, 1346 (1982). The effect mass of $20m_e$ quoted in the table includes a correction for the large *a b* mass anisotropy, by taking the geometric average: $\langle m_{ab}^*\rangle=\sqrt{2m_e\times 200m_e}$.
$H_{1/2}$	P. Garoche *et al.*, Phys. Rev. Lett. **49**, 1346 (1982).
$\lambda_{ab}(0)$	D. R. Harshman *et al.* (unpublished).
H_{c2}	P. Garoche *et al.*, Phys. Rev. Lett. **49**, 1346 (1982), perform this experiment with $\mathbf{H}_{\text{ext}}$ applied along c^*; D. Mailly *et al.*, J. Phys. (Paris) Colloq. **44**, C3-1037 (1983) and K. Murata *et al.* Jpn. J. Appl. Phys. **26**, Suppl. 26-3, 1357 (1984), indicate $H_{c2}\approx 0.16$ T. Since these measurements only extend down to 0.5 K, it is possible that the curve H_{c2} vs temperature turns upward below 0.5 K, in analogy with κ-$[BEDT\text{-}TTF]_2Cu[NCS]_2$, significantly increasing this estimation of H_{c2}.
19. A_3C_{60} (K_3C_{60}, . . . , Rb_2CsC_{60})	
Structure	P. W. Stephens *et al.*, Nature, (London) **351**, 632 (1991); R. M. Fleming *et al.*, *ibid.*, **352**, 701 (1991); see also Nature (London) **353**, 868(E) (1991). The structure parameters quoted in Table II correspond to Rb_3C_{60}.
α	C.-C. Chen and C. M. Lieber, J. Am. Chem. Soc. (to be published), obtain $\alpha=0.30\pm 0.06$ for K_3Co_{60}; A. P. Ramirez *et al.*, Phys. Rev. Lett. **68**, 1058 (1992), find $\alpha=0.38\pm 0.05$ for Rb_3C_{60}.
$\rho(0);\rho(T_c)$	A. Hebard *et al.*, Nature (London) **350**, 600 (1991).
Coherence effects	R. Tycko *et al.*, Phys. Rev. Lett. **68**, 1912 (1992), present data indicating the absence of a Hebel-Slichter anomaly in K_3C_{60}.
$\Delta C/T_c$	*x*
$H_{1/2}$	*x*
$\lambda_{ab}(0)$	Y. J. Uemura *et al.*, Nature (London) **352**, 605 (1991), give a value of 4800 Å for K_3C_{60}. Note, also, that there may be significant dirty-limit or finite-*l* corrections to this value. D. R. Harshman *et al.* (unpublished), obtain effective values of 5100 and 4400 Å for K_3C_{60} and Rb_3C_{60}, respectively, and discuss the question of dirty-limit superconductivity. Band-structure calculations by S. C. Erwin and W. E. Pickett, Science **254**, 842 (1991), suggest a clean-limit value of 1600 Å.
H_{c2}	K. Holczer *et al.*, Phys. Rev. Lett. **67**, 271 (1991); K. Holczer *et al.*, Science **252**, 1154 (1991), originally suggested $H_{c2}\approx 50$ T; more recent measurements, T. T. M. Palstra (private communication), suggest $H_c\sim 30$ T. Note, also, that there may be significant dirty-limit or finite-*l* corrections to this value.
20. KC_8	
Structure	G. S. Parry, Mater. Sci. Eng. **31**, 99 (1977).
α	*x*
$\rho(0);\rho(T_c)$	*x*
Coherence effects	*x*
$\Delta C/T_c$	*x*

APPENDIX TO TABLES I AND II (*Continued*).

$H_{1/2}$	x
$\lambda_{ab}(0)$	x
H_{c2}	x
21. $TaS_2(Py)_{1/2}$	
Structure	F. R. Gamble *et al.*, Science **174**, 493 (1971).
α	x
$\rho(0);\rho(T_c)$	Y. Kashihara *et al.*, J. Phys. Soc. Jpn. **46**, 1112 (1979). The slope between 3.5 and 4 K is zero.
Coherence effects	x
$\Delta C/T_c$	Y. Kashihara *et al.*, J. Phys. Soc. Jpn. **46**, 1112 (1979); R. E. Schwall *et al.*, J. Low Temp. Phys. **22**, 557 (1976).
$H_{1/2}$	x
$\lambda_{ab}(0)$	Y. Kashihara *et al.*, J. Phys. Soc. Jpn. **46**, 1112 (1979); R. E. Schwall *et al.*, J. Low Temp. Phys. **22**, 557 (1976).
H_{c2}	Y. Kashihara *et al.*, J. Phys. Soc. Jpn. **46**, 1112 (1979); R. E. Schwall *et al.*, J. Low Temp. Phys. **22**, 557 (1976).
22. $Ba_{0.6}K_{0.4}BiO_3$	
Structure	L. F. Schneemeyer *et al.*, Nature (London) **335**, 421 (1988).
α	C. K. Loong *et al.*, Phys. Rev. Lett. **66**, 3217 (1991).
$\rho(0);\rho(T_c)$	N. Savvides *et al.*, Physica C **171**, 181 (1990).
Coherence effects	x
$\Delta C/T_c$	J. E. Graebner *et al.*, Phys. Rev. B **39**, 9682 (1989).
$H_{1/2}$	J. E. Graebner *et al.*, Phys. Rev. B **39**, 9682 (1989).
$\lambda_{ab}(0)$	Y. J. Uemura *et al.*, Phys. Rev. Lett. **66**, 2665 (1991), show *s*-wave behavior but with a suppressed T_c.
H_{c2}	J. E. Graebner *et al.*, Phys. Rev. B **39**, 9682 (1989).
23. $BaPb_{0.75}Bi_{0.25}O_3$	
Structure	D. E. Cox and A. W. Sleight, in *Proceedings of the Conference on Neutron Scattering*, Gatlinberg, TN, 1976, edited by R. M. Moon (National Technical Information Service, Springfield, VA, 1976); D. E. Cox and A. W. Sleight, Solid State Commun. **19**, 969 (1976); D. E. Cox and A. W. Sleight, Acta Crystallogr. Sect. B **35**, 1 (1979).
α	B. Batlogg *et al.*, Phys. Rev. Lett. **61**, 1670 (1988).
$\rho(0);\rho(T_c)$	A. W. Sleight *et al.*, Solid State Commun. **17**, 27 (1975).
$\Delta C/T_c$	x
$H_{1/2}$	x
$\lambda_{ab}(0)$	D. R. Harshman *et al.*, (unpublished).
H_{c2}	B. Batlogg, Physica B **126**, 275 (1974); T. D. Thanh *et al.*, Appl. Phys. **22**, 205 (1980); K. Kitazawa *et al.*, Physica B **135**, 505 (1985).
24. $PbMo_6S_8$ (Chevrel)	
Structure	J. D. Jorgensen *et al.*, Phys. Rev. B **35**, 5365 (1987).
α	F. J. Culetto and F. Pobell, Phys. Rev. Lett. **40**, 1104 (1978), obtain $\alpha=0.27\pm0.04$ for $Mo_6Se_{7.6}$ (Mo isotope).
$\rho(0);\rho(T_c)$	R. Flükiger *et al.*, Mater. Res. Bull. **13**, 743 (1978); for radiation effects, see G. Adrian and H. Adrian, Z. Phys. B **67**, 75 (1987).
Coherence effects	x
$\Delta C/T_c$	J. Cors *et al.*, Physica B **165&166**, 1521 (1990).
$H_{1/2}$	J. Cors *et al.*, Physica B **165&166**, 1521 (1990).
$\lambda_{ab}(0)$	P. Birrer *et al.*, Hyperfine Interact. **63**, 103 (1990).
H_{c2}	J. Cors *et al.*, Physcia B **165&166**, 1521 (1990), derive their number from the field-dependence of T_c measured by specific heat.
25. UPt_3	
Structure	G. Aeppli *et al.*, Phys. Rev. Lett. **60**, 615 (1988).
α	x

APPENDIX TO TABLES I AND II (*Continued*).

$\rho(0);\rho(T_c)$	G. R. Stewart, J. Appl. Phys. **57**, 3049 (1985); Rev. Mod. Phys. **56**, 755 (1984).
Coherence effects	Y. Kohori *et al.*, J. Phys. Soc. Jpn. **57**, 395 (1988); for a review of NMR in heavy-fermion systems, see K. Asayama *et al.*, J. Magn. Magn. Mater. **76-77**, 449 (1988). The absence of the coherence peak in UPt_3 results from the *d*-wave nature of the ground-state wave function.
$\Delta C/T_c$	K. Hasselbach *et al.*, Phys. Rev. Lett. **63**, 93 (1989); E. Schuberth *et al.*, Physica C **162-164**, 415 (1989).
$H_{1/2}$	G. R. Stewart, J. Appl. Phys. **57**, 3049 (1985).
$\lambda_{ab}(0)$	C. Broholm *et al.*, Phys. Rev. Lett. **65**, 2062 (1990). This experiment was conducted in low field ($H_{ext}<200$ *G*), to circumvent problems associated with a reduced modulation effect, which can occur when the intervortex distance becomes comparable to $\xi_0(\approx 120\,\text{Å})$. The strong field-dependence observed for UPt_3 in the zero-temperature μ^+SR relaxation rate, $\sigma(0)$, is a clear signature of such an effect. In fact, the dependence of $\sigma(0)$ on magnetic field also provides a way of directly measuring ξ_0.
H_{c2}	B. S. Shivaram *et al.*, Phys. Rev. Lett. **57**, 1259 (1986).
26. Nb_3Sn	
Structure	S. Geller *et al.*, J. Am. Chem. Soc. **77**, 1502 (1955); B. T. Matthias *et al.*, Phys. Rev. **95**, 1435 (1954).
α	J. W. Garland, Jr. Phys. Rev. Lett. **11**, 114 (1963).
$\rho(0);\rho(T_c)$	T. P. Orlando *et al.*, Phys. Rev. B **19**, 4545 (1979).
Coherence effects	*x*
$\Delta C/T_c$	M. N. Khlopkin, Zh. Eksp. Teor. Fiz. **90**, 286 (1986) [Sov. Phys. JEPT **63**, 164 (1986)]; $\gamma(0)=0$—F. Hellman and T. H. Geballe, Phys. Rev. B **36**, 107 (1987).
$H_{1/2}$	M. N. Khlopkin, Zh. Eksp. Teor. Fiz. **90**, 286 (1986) [Sov. Phys. JEPT **63**, 164 (1986)].
$\lambda_{ab}(0)$	T. P. Orlando *et al.*, Phys. Rev. B **19**, 4545 (1979), estimated from H_{c2} measurements.
H_{c2}	T. P. Orlando *et.al.*, Phys. Rev. B **19**, 4545 (1979).

T_c for a set of $YBa_2Cu_3O_{7-\delta}$ films, indicating that the highest T_c coincides with the vanishing of the residual resistivity. The fact that $\rho(0)$ tends toward zero, coupled with the observed linear temperature dependence for $T>T_c$, is evidence that $\rho(T>T_c)$ is not dominated by impurity scattering.[20] For the quasi-1D organic superconductor, $[TMTSF]_2ClO_4$, $\rho(T>T_c)$ exhibits a nonlinear behavior, possibly related to its lower dimensionality.[21] Nonlinear behavior is also observed for $YBa_2Cu_3O_{6.67}$ ($T_c=60$ K) and $YBa_2Cu_4O_8$ (at ambient pressure), with $\rho(T>T_c)$ for both extrapolating to a nonzero residual resistivity $\rho(0)$.[22,23] Given the similarity observed in $\rho(T>T_c)$ for $[TMTSF]_2ClO_4$ and $YBa_2Cu_3O_{6.67}$, the nonlinear behavior observed may be reflecting the 1D character of the chains. The electron-doped cuprates show a roughly constant $\rho(T>T_c)$, possibly indicative of phase inhomogeneity, which is known to produce similar transport behavior in hole-doped cuprate superconductors. It is also worth noting that $\rho(T>T_c)$ for A_3C_{60} resembles that of the nonoptimal cuprates,[24] while $\rho(T>T_c)$ is constant for KC_8. The 3D $Ba_{1-x}(Pb,K)_xBiO_3$ systems, $TaS_2(Py)_{1/2}$, and Nb_3Sn also show a constant $\rho(T>T_c)$. Figure 3 shows examples of $\rho(T)$ for $YBa_2Cu_3O_7$ and κ-[BEDT-TTF]$_2$Cu[NCS]$_2$.[25,26]

The hydrostatic pressure-dependence of $\rho(T>T_c)$ could provide additional information regarding the bulk electronic properties. However, work done on $YBa_2Cu_3O_7$ (Ref. 27) has shown that increasing pressure reduces T_c and broadens the transition width ΔT_c, sug-

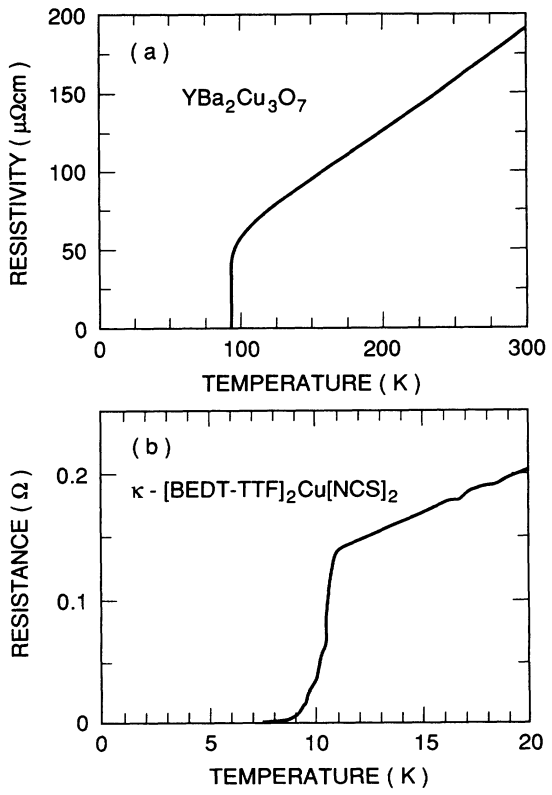

FIG. 3. Basal-plane $\rho(T)$, for single-crystal $YBa_2Cu_3O_7$ and $R(T)$ for κ-[BEDT-TTF]$_2$Cu[NCS]$_2$. Data taken from Refs. 25 and 26, respectively.

gesting an increasing disordering of the system. Similar studies of both $Bi_2Sr_2CaCu_2O_{8+\delta}$ and κ-[BEDT-TTF]$_2$Cu[NCS]$_2$,[28,29] tend to support the notion of pressure-induced disorder. In contrast, T_c actually increases for the $(R)Ba_2Cu_4O_8$ compounds, reaching a maximum of 107 K at about 10 GPa before decreasing again,[30] suggesting that the ambient-pressure materials of this type are nonoptimal. The strong pressure dependence may be due to a significant increase in m^*, E_F^{2D}, or n_{2D} accompanying the 25% reduction in the molar volume. For sintered powder samples, we obtain an estimate[31] for the single-crystal average *ab*-plane resistivity by dividing the measured resistivities by five.

(4) Coherence Effects. One of the hallmarks of BCS theory is the presence of coherence factors for effects having to do with the electron-lattice interaction. In the case of phonon-mediated *s*-wave pairing, these factors have a pronounced effect on ultrasonic attenuation and electromagnetic absorption, and give rise to the Hebel-Slichter T_1T anomaly in NMR.[4] For higher angular momentum pairing, the T_1T anomaly is suppressed, as in UPt_3 which exhibits *d*-wave characteristics. Even for conventional pairing, the coherence peak can be suppressed by magnetic scattering, while significant gap anisotropies and strong electron-phonon coupling may act to broaden the peak in the density of states. So far, no evidence of an NMR coherence peak or other coherence effect has been observed in the high-T_c cuprates, or in either κ-[BEDT-TTF]$_2$Cu[NCS]$_2$ or [TMTSF]$_2$ClO$_4$. Since the high-T_c cuprates and [BEDT-TTF]-based organics (preliminary μ^+SR measurements of [TMTSF-TTF]$_2$ClO$_4$ also suggest *s*-wave pairing) are known to be *s* wave, the possibility of magnetic scattering or spin-mediated pairing is small. Interestingly, recent NMR relaxation measurements[32] of K_3C_{60} give no indication of a Hebel-Slichter anomaly. An NMR experiment has not been performed on $Ba_{0.6}K_{0.4}BiO_3$ to our knowledge. Given its conventional isotope effect, resistivity, specific heat, and apparent *s*-wave character (see below), it would not be surprising if $Ba_{0.6}K_{0.4}BiO_3$, did not also have a conventional BCS case-II anomaly in the T_1-NMR. A peak in the real part of the high-frequency conductivity, similar to the coherence peak expected in an *s*-wave BCS superconductor, has been observed in $YBa_2Cu_3O_7$ by Nuss *et al.*[33] However, the absence of such a peak in the NMR relaxation rate suggests to these authors that its origin lies in a strongly temperature-dependent inelastic scattering rate rather than in coherence factors. Typical measurements of $1/T_1$ are presented in Fig. 4 for $YBa_2Cu_3O_7$ and κ-[BEDT-TTF]$_2$Cu[NCS]$_2$.[34,35] The peak observed for the latter sample is field dependent, and not associated with coherence factor effects.[36] We also note that while inelastic scattering can suppress the coherence terms in BCS theory, pair breaking associated with inelastic scattering is minimized for the optimized materials.

(5) Specific-heat anomaly, $\Delta C/T_c$. According to Eqs. (2) and (3), the specific-heat jump in 3D provides a measure of the product $m^*(n_{3D})^{1/3}$, while depending only on the 2D effective mass m_{ab}^*, and the average plane spacing

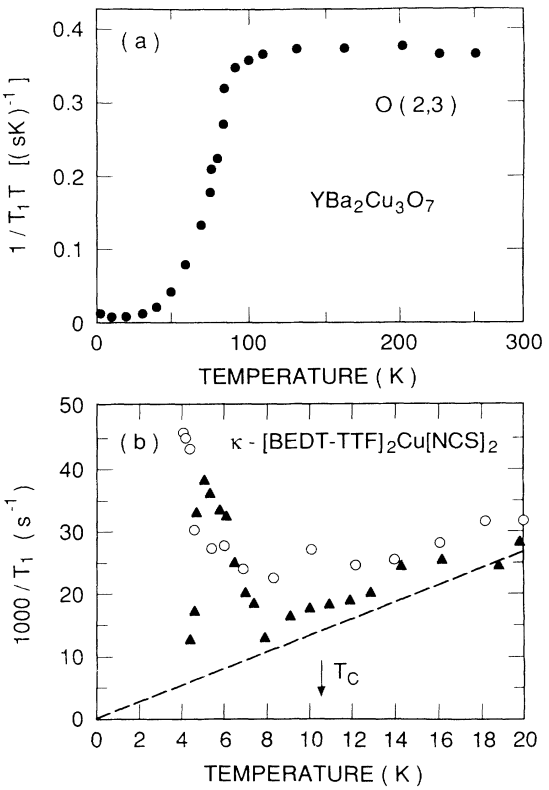

FIG. 4. NMR T_1T relaxation measurements in (a) $YBa_2Cu_3O_7$ [O(2,3) sites] and (b) κ-[BEDT-TTF]$_2$Cu[NCS]$_2$ (the solid symbols correspond to 0.33 T while the open symbols represent data taken at 6.3 T). The data taken are from Refs. 34 and 35 (Schweitzer *et al.*), respectively. The peak shown below T_c for κ-[BEDT-TTF]$_2$Cu[NCS]$_2$ is strongly field dependent and not associated with coherence factor effects.

δ, for two-dimensional systems. For quasi-1D materials, such as [TMTSF]$_2$ClO$_4$, we use Eq. (4) in combination with transfer integral calculations.[37] Unfortunately, $\Delta C/T_c$ is not always well defined and is subject to significant fluctuation effects.[38,39] Another important feature of the specific heat is the extrapolated *y* intercept of the linear term in $C/T, \gamma(0)$; a nonzero value of $\gamma(0)$ is generally recognized as indicating an incomplete transition to the superconducting state.[39] Since the strength of coupling is not known conclusively, the electronic contribution to C/T is extracted assuming weak coupling,[40] such that $1.43 = \Delta C/\gamma T_c$. We note that in doped $YBa_2Cu_3O_7$, $\Delta C/T_c$ decreases more rapidly than T_c with increased doping, in a manner consistent with disorder effects that are also reflected in ΔT_c, α, $\lambda(0)$, and/or $\rho(0)$. Figure 5 shows $\Delta C/T_c$ versus T_c for $YBa_2(Cu_{1-x}M_x)_3O_7$, with M = Fe or Zn. Due to possible mass renormalization, m_{ab}^* derived from specific-heat measurements may not be the same as that derived from band-structure or normal-state measurements.

(6) $H_{1/2}$. Unlike their conventional counterparts, which exhibit a rapid suppression in T_c with increasing field, $\Delta C/T_c$ for the high-T_c cuprates is seen to decrease rapidly with increasing field, while maintaining a near-

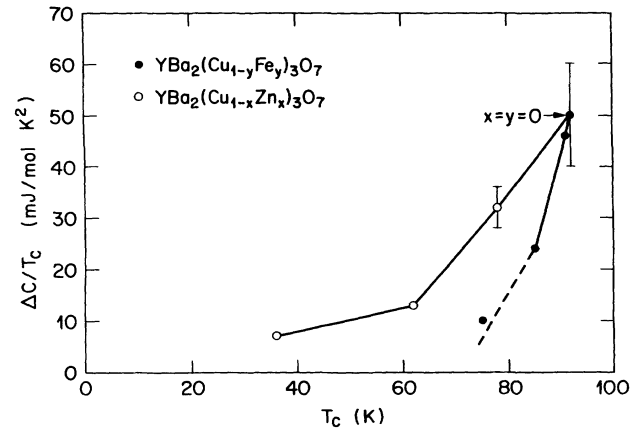

FIG. 5. The specific-heat anomaly, $\Delta C/T_c$, vs T_c for $YBa_2(Cu_{1-x}M_x)_3O_7$, with M=Fe and Zn. Data taken from Table I, see Appendix.

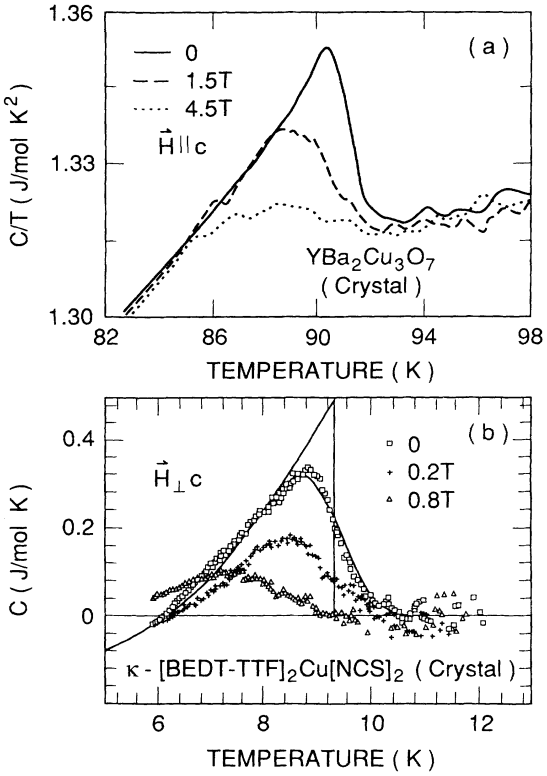

FIG. 6. Detail of the specific-heat jump $\Delta C/T_c$ for single-crystal $YBa_2Cu_3O_7$ and κ-[BEDT-TTF]$_2$Cu[NCS]$_2$. Data taken from Refs. 39 (Salamon *et al.*) and 41, respectively.

constant T_c.[41] In part, this unconventional field dependence can be understood in terms of the relatively high value and extreme anistropy of H_{c2} observed for the high-T_c cuprates. However, the more relevant quantity is the field dependence of the 2D fluctuation correlation length.[38] Given that the same behavior is also observed in the organic materials, κ-[BEDT-TTF]$_2$Cu[NCS]$_2$ and [TMTSF]$_2$ClO$_4$,[41,42] both having comparatively much lower H_{c2} values, we consider this type of field dependence characteristic of the high-T_c pairing mechanism. To quantify this effect, we define $H_{1/2}$ to be the field at which $\Delta C/T_c$ decreases to one-half of its zero-field value. Unfortunately, no data have been taken for the express purpose of measuring $H_{1/2}$ and we can only estimate it from the available measurements on $\Delta C/T_c$ taken at different fields. Figure 6 shows representative data for $YBa_2Cu_3O_7$ and κ-[BEDT-TTF]$_2$Cu[NCS]$_2$. Interestingly, $\Delta C/T_c$ for $Ba_{1-x}(Pb,K)_xBiO_3$, $PbMo_6S_8$, Nb_3Sn, and UPt_3 exhibits a conventional field dependence. No observation of a specific-heat jump $\Delta C/T_c$ has been reported for A_3C_{60}.

(7) Magnetic penetration depth, $\lambda_{ab}(0)$. The penetration depth $\lambda(T\rightarrow 0)$ reflects the ratio m^*/n_{3D}, and (if properly determined) is one of the most reliable experimental quantities relevant to the present subject. For 2D materials, we list in Table I the basal-plane penetration depth, denoted by $\lambda_{ab}(0)$ in the text. When available the values of $\lambda(0)$ given in Table I were extracted from bulk μ^+SR measurements in phase-pure samples. In the case of $Tl_2Ba_2CuO_6$, however, we use the value obtained from NMR, while H_{c2} measurements were used for $TaS_2(Py)_{1/2}$ and Nb_3Sn. The μ^+SR experiments are conducted on field cooling with the external field, $\mathbf{H}_{ext}$, applied perpendicular to the incident μ^+ spin direction. In the case of single crystals, $\lambda_{ab}(T)$ is obtained directly with $\mathbf{H}_{ext}$ applied parallel to the c axis, while for sintered materials, one measures a powder average, $\langle\lambda_{ab}(T)\rangle$, from which one can derive $\lambda_{ab}(T)$ by correcting for the effective-mass anisotropy m_c^*/m_{ab}^*.[14,43] As detailed in previous work,[7,14,44] $\lambda_{ab}(T)$ is determined from the relaxation of the ensemble μ^+-spin polarization, with $\mathbf{H}_{ext}$ chosen to satisfy the simple London picture, $H_{c1}\ll H_{ext}\ll H_{c2}$, such that the vortex lattice spacing is small compared to $\lambda_{ab}(T)$. Under such conditions, the μ^+-spin relaxation rate is expected to be independent of H_{ext}, and directly related to the second moment of the internal field distribution $\langle(\Delta B)^2\rangle$. For a perfect triangular lattice, $\langle(\Delta B)^2\rangle$ is related to λ (in the zero-field limit) via the equation[45]

$$\langle(\Delta B)^2\rangle-\langle B^2\rangle=0.003\,71\frac{\phi_0^2}{\lambda^4}\ , \tag{7}$$

where ϕ_0 ($=2.068\times10^{-7}$ G cm^2) is the magnetic flux quantum. Implicit in Eq. (7), however, are the assumptions that the vortices are static and form lines parallel to $\mathbf{H}_{ext}$, both of which can be violated in cases of extreme anisotropy. The internal field distribution, $\eta(B)$, associated with the induced vortex lattice is obtained directly via Fourier transformation of the measured μ^+SR time spectra. Representative measurements of $\lambda_{ab}(T)$ for single-crystal $YBa_2Cu_3O_7$ and κ-[BEDT-TTF]$_2$Cu[NCS]$_2$ are shown in Fig. 7.[14,46] In the absence of vortex-line motion, which tends to narrow and symmetrize $\eta(B)$,[47] the single-crystal and sintered powder distributions are both asymmetric and qualitatively different.[48] Thus the relationship between the μ^+SR relaxation function, $G_{xx}(t)$, and $\lambda_{ab}(T)$ is generally more complex than would

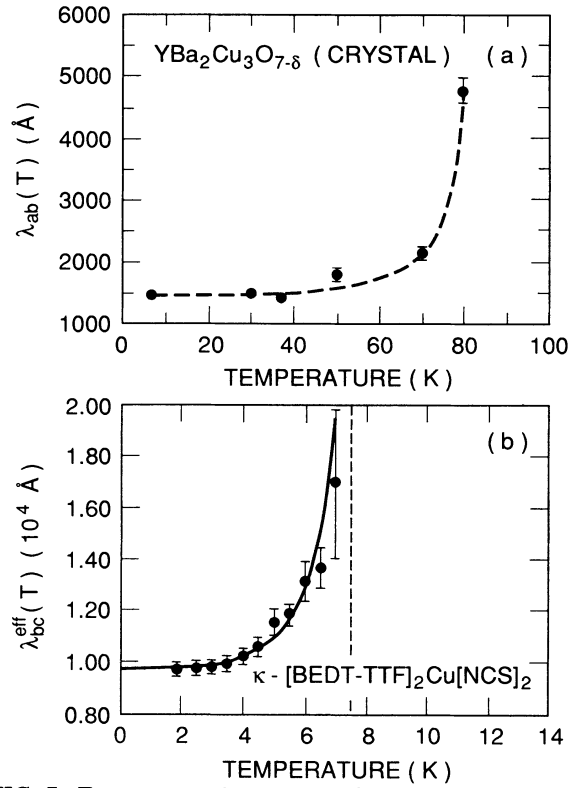

FIG. 7. Temperature dependence of the basal-plane penetration depth $\lambda_{ab}(T)$ for single-crystal $YBa_2Cu_3O_7$ and κ-[BEDT-TTF]$_2$Cu[NCS]$_2$. Data taken from Refs. 14 and 46, respectively.

be implied by simply assuming a Gaussian relaxation function, i.e., $G_{xx}(t)=\exp(-\sigma^2t^2)$. The more recent work[47] appropriately models $\eta(B)$, thus reducing the systematic errors arising from such factors as variable anisotropy, flux-line motion, and longitudinal disorder.

It is presently well established that the cuprate superconductors exhibit bulk superconductivity over a limited stoichiometric range. At optimal stoichiometry materials can be phase pure, but as one moves away from optimum, microscopic electronic inhomogeneities are induced, and further deviations from optimum lead to phase separation.[49] Such inhomogeneities can cause a reduction in l (along with changes in other transport properties), thereby moving the material closer to the "dirty limit." The effect of disorder on the penetration depth is most evident in the $La_{2-x}Sr_xCuO_{4-\delta}$ series, in which μ^+SR measurements exhibit a significant departure from s-wave behavior, indicative of electronic inhomogeneities; for $x=0.075$ and 0.25, two μ^+SR signals are observed, indicating phase separation. A similar behavior is also seen in poor quality "nominally 60-K" $YBa_2Cu_3O_{7-\delta}$,[50] where the temperature-dependence of $\sigma(T)$ again indicates phase and/or electronic inhomogeneity.[49] In homogeneous, phase-pure samples, both the 90-K and 60-K phases of $YBa_2Cu_3O_{7-\delta}$ exhibit behavior consistent with conventional s-wave pairing.[7,14] Thus, a clean-limit analysis which neglects l compared to ξ_0 should be considered only for the optimized compounds in the various families, with the relevant selection criteria being the absence of multiple μ^+SR signals, sharp magnetic transitions, high Meissner fractions, low residual resistivities, and the absence of anomalous temperature dependences in the published data that would be indicative of deviations from s-wave behavior or complex vortex dynamics. It has been shown that the dependence of T_c on $\lambda^{-2}(0)$ becomes linear as T_c is lowered by altering the carrier density from its optimum value in a single compound.[50,51] Examples of such measurements taken from the Table I entries for $(Y_{1-x}Pr_x)Ba_2Cu_3O_7$ and $La_{2-x}Sr_xCuO_4$ are shown in Fig. 8. However, the nonoptimal measurements of T_c versus $E_F^{\rm eff}$ [defined in Eq. (8b) below] shown in Fig. 8 cannot be correctly interpreted as implying a linear variation of T_c with $E_F^{\rm 2D}$ (dashed line, with slope $=15$) because, as we see from Table I, the residual resistivity $\rho(0)$, the isotope-effect exponent α, and/or ΔT_c, increase significantly as one departs from the carrier concentration associated with the highest T_c. Thus, $E_F^{\rm eff}=E_F^{\rm 2D}$ only for the materials optimized for minimum disorder effects and highest T_c, in which case T_c may in fact be proportional to $E_F^{\rm 2D}$ (solid line in Fig. 8, with slope $=25$). We also note that the transition widths ΔT_c are a stronger function of doping for $La_{2-x}Sr_xCuO_4$ as compared to $(Y_{1-x}Pr_x)Ba_2Cu_3O_7$, suggesting a more homogeneous disorder for the latter (i.e., a sharp transition width does not guarantee optimal superconductivity).

(8) Upper Critical Field, $H_{c2}(0)$. The upper critical fields in Table I are obtained from the derivative of T_c with respect to H, $H_{c2}(0)\approx T_c(H=0)/(dT_c/dH)$, unless direct measurements are available. As one might expect, the extrapolation error increases with $H_{c2}(0)$.

Table II: Structural parameters

The lattice constants, relevant atomic spacings, volumes, and densities are listed in Table II. For layered materials, the average plane spacing δ is defined in Eq. (3). However, the distance between paired conducting

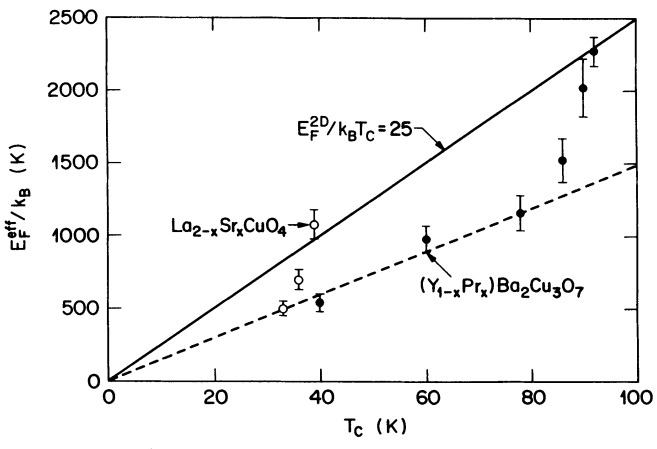

FIG. 8. The effective 2D Fermi energy, $E_F^{\rm eff}$ [derived from the inverse square of the effective penetration depth $\lambda_{ab}^{\rm eff}(0)$], vs T_c for $(Y_{1-x}Pr_x)Ba_2Cu_3O_7$ and $La_{2-x}Sr_xCuO_4$. The solid line corresponds to Eq. (11), with $\beta_3^{-1}=25$ and the dashed line to intrinsic disorder [see Eq. (8)]. Data taken from Tables I and III.

sheets d requires some discussion. For many of the bilayer materials, there is no ambiguity, and d is the spacing between the two closely spaced layers. The values of δ and d for κ-[BEDT-TTF]$_2$Cu[NCS]$_2$ and [TMTSF]$_2$ClO$_4$ are chosen to be equal to the distance between the anion layers and chains, respectively. In the case of κ-[BEDT-TTF]$_2$Cu[NCS]$_2$, the Cu[NCS]$_2$ anions are spaced a distance 15.24 Å apart along the a axis,[52] while the ClO$_4$ chains in [TMTSF]$_2$ClO$_4$ are spaced every 13.275 Å along the c axis.[53] To contrast with the behavior of 2D systems, we also include 3D materials with d chosen to be equal to a (here, a is the lattice constant), although it is not obvious what (if any) length scale is appropriate. Given this assignment, we are able to calculate supposititious "2D" quantities (denoted parenthetically in the tables) for the 3D materials.

Several of the materials, namely the 60-K YBa$_2$Cu$_3$O$_{6.67}$, the single-layer Tl-based materials, and the three-layer compounds, have a complex geometry and charge distribution that makes it difficult to decide on the appropriate interlayer spacing without further experiments or calculations. For low carrier densities coupling between a closely spaced (i.e., ~3 Å) pair of conducting sheets might not be possible. We suggest the 60-K YBa$_2$Cu$_3$O$_{6.67}$ may be such a case, where the coupling occurs between the CuO$_2$ double layers (i.e., $d=c$). However, the chain structures may contain a significant number of mobile carriers, and possibly contribute to the superfluid density. While we assume d for the single-layer Tl-based materials (points No. 9 and No. 12) to be equal to the spacing between CuO$_2$ layers, the metallic TlO$_2$ planes may also be superconducting,[54] reducing both δ and d by a factor of 2. For those compounds having three adjacent CuO$_2$ layers, the center plane, having no apical oxygens, might contribute significantly less to the superfluid carrier density as compared to the outer two planes. A simplified electrostatic model for the distribution of holes among different CuO$_2$ planes[55] assigns about 10% of the holes to the center plane, while NMR measurements[56] suggest about 29%. We assume that all the carriers are on the two outer planes. The "correct" assignment for d for all these examples may well be more complex.

OPTIMIZATION AND DISORDER

Using the information in Tables I and II, we derive in Table III several quantities of relevance to a 2D interlayer-coupled system based on Eqs. (1)–(6): n_{3D}, n_{2D}, m^*/m_e, E_F^{3D}/k_B, E_F^{2D}/k_B, the sheet resistance $R(T_c)$, and the characteristic field H_0. Here we have introduced two new parameters: the sheet resistance of a single conducting plane, $R(T)=\rho(T)/\delta$, and the characteristic field, $H_0(\propto H_{c2})$, which we derive from $\Delta C/T_c$ and $\lambda_{ab}(0)$ as defined below in Eq. (17). Correlations shedding light on the superconducting mechanism would most likely occur between materials free of extrinsic effects. From the discussion of measurements above, the concept of an ideal or optimum high-T_c superconductor appears to have some basis, with the ideal high-T_c material characterized by a full Meissner fraction and

(1) A normal-state resistivity $\rho(T>T_c)$, which is proportional to T, having an extrapolated zero-temperature intercept $\rho(0)=0$.

(2) A suppressed isotope effect, i.e., small exponent, α.

(3) A well-defined zero-field specific-heat jump at T_c, $\Delta C/T_c$, and a near zero extrapolated C/T.

(4) An anomalously strong field dependence of $\Delta C/T_c$.

(5) The absence of coherence factor effects such as the Hebel-Slichter NMR T_1T anomaly.

(6) A basal-plane penetration depth $\lambda_{ab}(T)$, with a temperature dependence indicative (in the absence of vortex motion or disorder) of s-wave pairing.

Not all of the materials and stoichiometries listed in the tables can be considered optimal. As we have seen in Figs. 5 and 8, disorder decreases $\Delta C/T_c$ while increasing $\lambda_{ab}(0)$. Estimates of m_{ab}^*, E_F^{2D}, and $n_{2D}\propto m_{ab}^* E_F^{2D}$ obtained for the nonoptimal materials must therefore be considered lower limits. In other words, it is not that n_{2D} and m_{ab}^* have unreasonably small values in these cases, but rather that they cannot be reliably determined in the presence of enhanced disorder effects associated with nonoptimal samples.

The effect of disorder on the measured penetration depth can be most easily understood by considering the dirty limit. Using the definition $\xi_0=\hbar v_F/\pi\Delta_0$, where v_F is the Fermi velocity and Δ_0 the zero-temperature gap, and making a specific calculation for weak coupling, $\Delta_0=1.76k_BT_c$, we obtain from Eq. (1),[57]

$$\lambda_{\rm eff}^2(0)\approx\lambda_L^2(0)+\frac{\hbar c^2}{1.76\times4\pi^2}\frac{\rho_d}{k_BT_c}\ , \tag{8a}$$

where ρ_d is the component of the basal-plane resistivity due to disorder, and should be the same order of magnitude as the residual 2D resistivity, $\rho(0)$, extrapolated to $T=0$. Dividing by the average spacing δ, and noting

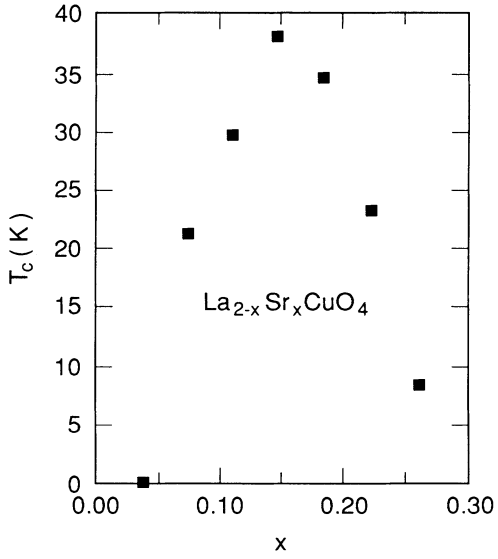

FIG. 9. The superconducting transition temperature, T_c, vs strontium concentration for $La_{2-x}Sr_xCuO_4$. Data taken from Ref. 17.

TABLE III. Relevant derived quantities, calculated from the information in Tables I and II. We note that for $YBa_2Cu_3O_{6.67}$ (point no. 3), n_{3D}, n_{2D}, and the sheet resistances, are calculated for double layers, while the value for E_F^{2D} is calculated for a single sheet.

No.	Compound	n_{3D} (10^{21} cm^{-3})	n_{2D} (10^{14} cm^{-2})	m^*/m_e	E_F^{3D}/k_B (K)	E_F^{2D}/k_B (K)	R(0) ; R(T_c) (Ω)	H_o (Tesla)
1.	$La_{1.9}Sr_{0.1}CuO_4$	~0.5	~0.4	~2.0	–	510±50	x	x
	$La_{1.875}Sr_{0.125}CuO_4$	~1.0	~0.6	~2.6	–	710±70	x	x
	$La_{1.85}Sr_{0.15}CuO_4$	5.2±0.8	3.4±0.5	8.6±1.0	–	1090±100	0 ; 500±90	4.6±0.6
	$La_{1.775}Sr_{0.225}CuO_4$	x	x	~2.6	–	x	x	x
	$La_{1.725}Sr_{0.175}CuO_4$	x	x	~0.9	–	x	x	x
2.	$La_{1.6}Sr_{0.4}CaCu_2O_6$	x	x	x	–	x	x	x
3.	$YBa_2Cu_3O_{6.67}$	1.1±0.4	1.3±0.5	2.6±1.0	–	710±70	x ; 535±70	2.5±1.0
4.	$YBa_2Cu_3O_7$	16.9±3.4	9.9±2.0	12.0±2.4	–	2290±100	0 ;685±85	16.5±3.4
	$HoBa_2Cu_3O_7$	x	x	x	–	x	x ; x	x
	$PrBa_2Cu_3O_7$	x	x	x	–	x	x ; x	x
	$(Y_{0.95}Pr_{0.05})Ba_2Cu_3O_7$	x	x	x	–	2040±200	855 ; 1700	x
	$(Y_{0.9}Pr_{0.1})Ba_2Cu_3O_7$	x	x	x	–	1530±150	855 ; 1700	x
	$(Y_{0.8}Pr_{0.2})Ba_2Cu_3O_7$	x	x	x	–	1170±120	1700 ; 2400	x
	$(Y_{0.7}Pr_{0.3})Ba_2Cu_3O_7$	x	x	x	–	990±90	4300 ; 4800	x
	$(Y_{0.6}Pr_{0.4})Ba_2Cu_3O_7$	x	x	x	–	550±60	5100 ; 5700	x
	$YBa_2(Cu_{0.99}Fe_{0.01})_3O_7$	x	x	11.0	–	x	x ; x	x
	$YBa_2(Cu_{0.975}Fe_{0.025})_3O_7$	x	x	5.7	–	x	x ; x	x
	$YBa_2(Cu_{0.95}Fe_{0.05})_3O_7$	x	x	2.4	–	x	x ; x	x
	$YBa_2(Cu_{0.99}Zn_{0.01})_3O_7$	x	x	7.7±1.0	–	x	x ; x	x
	$YBa_2(Cu_{0.975}Zn_{0.025})_3O_7$	x	x	3.1	–	x	2570 ; 3420	x
	$YBa_2(Cu_{0.95}Zn_{0.05})_3O_7$	x	x	x	–	x	4110 ; 5140	x
5.	$YBa_2Cu_4O_8$ (ambient press.)	2.8±0.44	1.9±0.3	3.8±0.5	–	1360±140	x ; x	6.7±1.1
	$YBa_2Cu_4O_8$ (10 GPa)	x	x	x	–	x	x ; x	x
	$HoBa_2Cu_4O_8$ (ambient press.)	~1.3	~0.9	~1.2	–	2070±200	1470 ; 5870	~1.4
6.	$Bi_2Sr_2CuO_{6\pm\delta}$	x	x	x	–	x	825 ; 900	x
	$Bi_2(Sr_{1.6}La_{0.4})CuO_{6+\delta}$	1.17±0.33	1.44±0.41	x	–	x	2610 ; 2940	x
	$(Bi,Pb)_2(Sr_{1.75}La_{0.25})CuO_6$	0.69±0.14	0.84±0.17	x	–	x	x	x
	$(Bi,Pb)_2(Sr_{1.8}Pr_{0.2})CuO_6$	0.57±0.11	0.70±0.14	x	–	x	x	x
	$(Bi,Pb)_2(Sr_{1.75}Nd_{0.25})CuO_6$	0.75±0.15	0.92±0.18	x	–	x	x	x
7.	$Bi_2Sr_2CaCu_2O_8$ (no-anneal)	3.5±1.8	2.7±1.4	7.8±2.4	–	970±390	0 ; 490±26	24±12
	$Bi_2Sr_2CaCu_2O_{8+\delta}$ (O_2 annealed)	x	x	x	–	x	x ; x	x
8.	$Bi_2Sr_2Ca_2Cu_3O_{10}$	x	x	4.4±1.2	–	x	0 ; <650	x
	$(Bi_{1.6}Pb_{0.4})Sr_2Ca_2Cu_3O_{10}$	3.4±1.2	3.2±1.1	7.8±1.9	–	1140±270	0 ; x	29±10
9.	$Tl_2Ba_2CuO_6$	x	x	x	–	3150±370	345 ; 860	x
10.	$Tl_2Ba_2CaCu_2O_8$	4.9±1.5	3.6±1.1	8.4±2.4	–	1180±110	0±20 ; 4100±1100	26±8
11.	$Tl_2Ca_2Ba_2Cu_3O_{10}$	4.2±1.5	3.8±1.3	5.7±1.9	–	1830±190	220 ; 925	18±6
12	$(Tl_{0.7}Cd_{0.3})BaLaCuO_5$	x	x	x	–	x	x	x
13.	$(Tl_{0.5}Pb_{0.5})Sr_2CaCu_2O_7$	2.8±0.5	1.7±0.3	3.2±0.5	–	1440±140	x ; x	5.3±1.0
	$(Tl_{0.5}Pb_{0.5})Sr_2(Ca_{0.8}Y_{0.2})Cu_2O_7$	x	x	5.5±0.5	–	x	0 ; 4130	x
14.	$(Tl_{0.5}Pb_{0.5})Sr_2Ca_2Cu_3O_9$	x	x	x	–	2410±240	x ; x	x
15.	$Pb_2(Y_{1-x}Ca_x)Sr_2Cu_3O_8$	x	x	x	–	x	635 ; 3180	x
16.	$(Nd_{2-x}Ce_x)CuO_4$	x	x	~0.4*	–	x	4140 ; 4140	x
17.	κ-[BEDT-TTF]$_2$Cu[NCS]$_2$	0.31±0.09	0.47±0.13	6.2±0.6	–	213±57	~0 ;2160±330	1.2±0.3
18.	$[TMTSF]_2ClO_4$	0.38±0.17	0.5±0.22	20±5	–	72±24	x ; x	0.15±0.07
19.	A_3C_{60} (K_3C_{60},...,Rb_2CsC_{60})	x	x	x	x	–	x ; x	x
20.	KC_8	x	x	x	–	x	x ; x	x
21.	$TaS_2(Py)_{1/2}$	12±3.6	14.2±4.4	23±5	–	1710±360	x ; x	0.058±0.018
22.	$Ba_{0.6}K_{0.4}BiO_3$	0.57±0.09	(0.24±0.04)	2.4±0.3	1210±120	–	(47k ; 47k)	0.76±0.16
23.	$BaPb_{0.75}Bi_{0.25}O_3$	0.12±0.015	(0.10±0.01)	4.2±0.4	242±20	–	(3940 ; 3940)	0.79±0.13
24.	$PbMo_6S_8$ (Chevrel)	1.0±0.27	(0.65±0.18)	2.6±0.4	1640±370	–	(770 ; 1390)	0.085±0.030
25.	UPt_3	7.8±1.0	(3.83±0.49)	135±17	124±5	–	(4.1 ; 10)	0.11±0.02
26.	Nb_3Sn	47±5	(24.7±2.8)	6.8±0.6	8100±620	–	(170 ; 170)	0.10±0.02

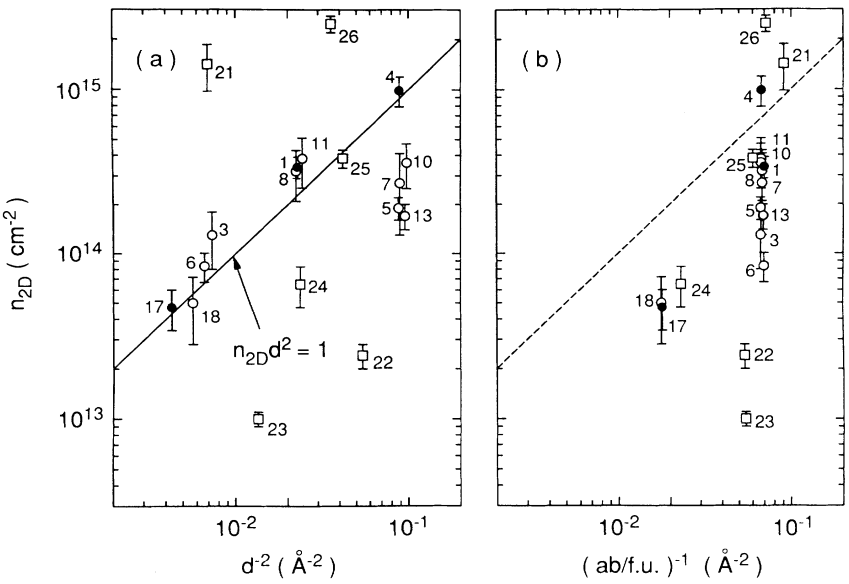

FIG. 10. The 2D carrier density, n_{2D}, vs (a) the inverse square of the interplanar distance, d^{-2}, and (b) the inverse of the area associated with each planar copper atom; for noncuprates, we use the area of the unit cell per formula unit. The solid circles represent data for materials having unambiguous geometries and that reasonably satisfy the criteria for sample phase-purity and minimum disorder effects, and the solid line corresponds to Eq. (9) for $\beta_1 = 1$. Data taken from Tables I–III, see the Appendix.

that the sheet resistance of a single plane is $R = \rho/\delta$, Eq. (8a) becomes

$$\frac{4e^2}{\hbar^2 c^2}\frac{\lambda_{\rm eff}^2(0)}{\delta} \equiv \frac{1}{E_F^{\rm eff}} = \frac{1}{E_F^{\rm 2D}} + \frac{2}{1.76\pi}\frac{R_d/R_K}{k_B T_c} , \quad (8b)$$

where we have used the expression for $E_F^{\rm 2D}$ in Eq. (5) and R_K ($=h/e^2=25812.8\ \Omega$) is the von Klitzing quantum-Hall-effect resistance.[58] When the two terms in Eq. (8) become comparable, one predicts a significant difference between $E_F^{\rm eff}$ and $E_F^{\rm 2D}$. From other measurements,[17,49] we also know that as one varies the carrier concentration, T_c goes through a maximum, exhibiting a quasiparabolic dependence on $E_F^{\rm 2D}$ (i.e., on $x \propto n_{2D}$) as shown in Fig. 9 for $La_{1-x}Sr_xCuO_4$. The Meissner fraction was also seen to peak at $x = 0.15$, and fall off rapidly with x away from this optimum value.[49] Thus, rather than being intrinsic to phase-pure optimal superconductivity, the linear dependence of T_c with $E_F^{\rm eff}$ in Fig. 8 instead reflects the presence of disorder, the effect of which increases and quickly saturates as one departs from optimum doping; since $E_F^{\rm 2D}$ decreases only slowly while T_c falls rapidly, we are left with a linear dependence of T_c on $E_F^{\rm eff}$ as $T_c \to 0$. This "disorder line" is represented by the dashed line (with slope = 15) in Fig. 8, and is the same line that has been misinterpreted as being intrinsic to superconductivity in Refs. 50 and 51. While the possibility of an optimal A_3C_{60} compound might be suggested by the strong dependence of T_c on the intercalate ($T_c = 19.3$ and 31.3 for K_3C_{60} and Rb_2CsC_{60}, respectively), it appears that T_c is actually changing with the lattice constant as expected for phonon-mediated pairing.[59] Although measurements of $\lambda(T)$ for K_3C_{60} indicate s-wave pairing,[60] resistivity measurements do not yet provide unambiguous information regarding the mean free path. Normal-state susceptibility and critical-field measurements of $K_{3-x}Rb_xC_{60}$ films characterize this material to be in the extreme dirty limit, with a mean free path of ~ 10 Å.[61] Thus, the measured $\lambda(0)$ may not reflect the true electronic state of K_3C_{60}.

An interesting possibility raised above is that there exists in the high-T_c cuprates a certain degree of intrinsic crystalline disorder that is more or less independent of doping, and which is sufficient in the absence of other effects to dominate the penetration depth and quench the specific-heat jump at T_c. It may be that the carriers responsible for superconductivity become insensitive to both impurity and phonon scattering at the optimal value of n_{2D}. If this same insensitivity to disorder holds even above T_c for these compounds, we would have a common explanation for the zero-resistivity intercept, the absence of an isotope effect, the maximum in $\Delta C/T_c$, and the minimum in $\lambda_{\rm eff}^2(0)$ exhibited by the optimally doped materials.

If there exists a set of criteria characterizing ideal high-T_c superconductivity, then it is natural to suppose that various ideal materials should have similar electronic properties; thus one might expect equal values for selected dimensionless ratios. For the convenience of the reader, we list in Table IV the following dimensionless quantities which could be significant for 2D (layered) systems: $n_{2D}d^2$, $m^*d/m_e a_0$, $E_F/k_B T_c$ (3D or 2D, whichever is appropriate), $H_0/H_{1/2}$, $R(T_c)/R_K$, and $m^* dR_K/m_e a_0 R(T_c)$. These quantities are represented graphically in Figs. 10–13, with the points labeled according to the numbering in Tables I–IV. The circles (numbers 1–18) represent the layered materials that might be considered high-T_c in nature; the high-T_c materials having optimized parameters and unambiguous geometries are denoted by filled circles, while nonoptimal

TABLE IV. Dimensionless quantities derived from Tables II and III. Note that for $YBa_2Cu_3O_{6.67}$, $n_{2D}d^2$ is calculated for a double layer, while E_F/k_BT_c is derived for a single conducting sheet.

No.	Compound	$n_{2D}d^2$	m^*d/m_ea_o	E_F/k_BT_c	$H_o/H_{1/2}$	$R(T_c)/R_K$	$m^*d\,R_K/m_ea_oR(T_c)$
1.	$La_{1.9}Sr_{0.1}CuO_4$	x	x	15.5±1.5	x	x	x
	$La_{1.875}Sr_{0.125}CuO_4$	x	x	19.7±2.0	x	x	x
	$La_{1.85}Sr_{0.15}CuO_4$	1.48±0.22	108±12	27.9±2.6	x	0.019±0.004	5680±1360
	$La_{1.775}Sr_{0.225}CuO_4$	x	x	x	x	x	x
	$La_{1.725}Sr_{0.275}CuO_4$	x	x	x	x	x	x
2.	$La_{1.6}Sr_{0.4}CaCu_2O_6$	x	x	x	x	x	x
3.	$YBa_2Cu_3O_{6.67}$	1.83±0.69	58±22	11.8±1.2	x	0.021±0.003	2760±1120
4.	$YBa_2Cu_3O_7$	1.11±0.23	76±15	24.9±1.1	5.5±2.2	0.027±0.003	2815±640
	$HoBa_2Cu_3O_7$	x	x	x	x	x	x
	$PrBa_2Cu_3O_7$	x	x	x	x	x	x
	$(Y_{0.95}Pr_{0.05})Ba_2Cu_3O_7$	x	x	22.1±2.2	x	x	x
	$(Y_{0.9}Pr_{0.1})Ba_2Cu_3O_7$	x	x	17.8±1.7	x	x	x
	$(Y_{0.8}Pr_{0.2})Ba_2Cu_3O_7$	x	x	15.0±1.5	x	x	x
	$(Y_{0.7}Pr_{0.3})Ba_2Cu_3O_7$	x	x	16.5±1.5	x	x	x
	$(Y_{0.6}Pr_{0.4})Ba_2Cu_3O_7$	x	x	13.8±1.5	x	x	x
	$YBa_2(Cu_{0.99}Fe_{0.01})_3O_7$	x	70	x	x	x	x
	$YBa_2(Cu_{0.975}Fe_{0.025})_3O_7$	x	36	x	x	x	x
	$YBa_2(Cu_{0.95}Fe_{0.05})_3O_7$	x	15	x	x	x	x
	$YBa_2(Cu_{0.99}Zn_{0.01})_3O_7$	x	49±6	x	x	x	x
	$YBa_2(Cu_{0.975}Zn_{0.025})_3O_7$	x	20	x	x	x	x
	$YBa_2(Cu_{0.95}Zn_{0.05})_3O_7$	x	11	x	x	x	x
5.	$YBa_2Cu_4O_8$ (ambient press.)	0.21±0.03	24±3	17.0±1.7	x	x	x
	$YBa_2Cu_4O_8$ (10 GPa)	x	x	x	x	x	x
	$HoBa_2Cu_4O_8$ (ambient press.)	~0.1	~7	25.8±2.5	x	~0.23	~30
6.	$Bi_2Sr_2CuO_{6\pm\delta}$	x	x	x	x	x	x
	$Bi_2(Sr_{1.6}La_{0.4})CuO_{6+\delta}$	2.16±0.61	x	x	x	x	x
	$(Bi,Pb)_2(Sr_{1.75}La_{0.25})CuO_6$	1.27±0.25	x	x	x	x	x
	$(Bi,Pb)_2(Sr_{1.8}Pr_{0.2})CuO_6$	1.03±0.20	x	x	x	x	x
	$(Bi,Pb)_2(Sr_{1.75}Nd_{0.25})CuO_6$	1.35±0.26	x	x	x	x	x
7.	$Bi_2Sr_2CaCu_2O_8$ (no-anneal)	0.27±0.14	49±15	10.9±4.4	x	0.019±0.001	2580±800
	$Bi_2Sr_2CaCu_2O_{8+\delta}$ (O_2 annealed)	x	x	x	x	x	x
8.	$Bi_2Sr_2Ca_2Cu_3O_{10}$	x	55±15	x	x	<0.025	<2200
	$(Bi_{1.6}Pb_{0.4})Sr_2Ca_2Cu_3O_{10}$	1.44±0.50	98±25	10.7±2.5	x	x	x
9.	$Tl_2Ba_2CuO_6$	x	x	37.1±4.4	x	0.033	x
10.	$Tl_2Ba_2CaCu_2O_8$	0.36±0.11	51±15	11.9±1.1	x	0.16±0.04	320±120
11.	$Tl_2Ca_2Ba_2Cu_3O_{10}$	1.56±0.54	70±23	14.6±1.5	x	0.036	1940
12.	$(Tl_{0.7}Cd_{0.3})BaLaCuO_5$	x	x	x	x	x	x
13.	$(Tl_{0.5}Pb_{0.5})Sr_2CaCu_2O_7$	0.17±0.03	20±3	18.0±1.8	x	x	x
	$(Tl_{0.5}Pb_{0.5})Sr_2(Ca_{0.8}Y_{0.2})Cu_2O_7$	x	34±3	x	x	0.16	x
14.	$(Tl_{0.5}Pb_{0.5})Sr_2Ca_2Cu_3O_9$	x	x	19.7±2.0	x	x	x
15.	$Pb_2(Y_{1-x}Ca_x)Sr_2Cu_3O_8$	x	x	x	x	0.12	x
16.	$(Nd_{2-x}Ce_x)CuO_4$	x	~4	x	x	0.16	~25
17.	κ-[BEDT-TTF]$_2$Cu[NCS]$_2$	1.10±0.31	177±18	20.2±5.4	6.0±3.5	0.084±0.013	2110±390
18.	$[TMTSF]_2ClO_4$	0.88±0.39	500±125	60±20	7.5±3.8	x	x
19.	A_3C_{60} (K_3C_{60},...,Rb_2CsC_{60})	x	x	x	x	x	x
20.	KC_8	x	x	x	x	x	x
21.	$TaS_2(Py)_{1/2}$	20.5±6.3	525±117	500±105	x	x	x
22.	$Ba_{0.6}K_{0.4}BiO_3$	(0.044±0.007)	(19.6±2.9)	37.8±3.7	~0.13	(1.8)	(10.9)
23.	$BaPb_{0.75}Bi_{0.25}O_3$	(0.074±0.01)	(69.3±7.7)	22±1.8	x	(0.15)	(460)
24.	$PbMo_6S_8$ (Chevrel)	(0.27±0.08)	(31.7±6.6)	137±31	0.01±0.003	(0.056)	(587)
25.	UPt_3	(1.87±0.24)	(1243±155)	234±10	~0.18	(0.0004)	(3108k)
26.	Nb_3Sn	(13.1±1.5)	(67.7±6.9)	453±35	0.013±0.002	(0.007)	(9670)

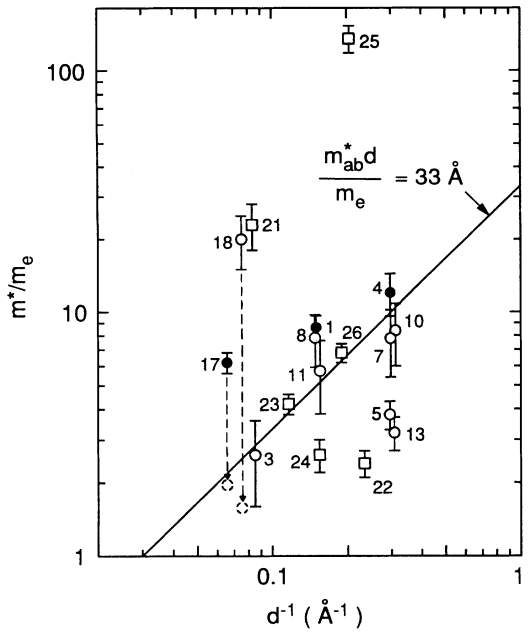

FIG. 11. The effective mass, m^*/m_e, vs the inverse of the interplanar distance, d^{-1}. The solid circles represent data for materials having unambiguous geometries and that reasonably satisfy the criteria for sample phase-purity and minimum disorder effects. The line corresponds to Eq. (10) with the proportionality constant chosen to agree with points No. 1 and No. 4. The dashed lines and circles show where the points No. 17 and No. 18 might be if we correct for the difference in the average dielectric constant from point No. 4. For point No. 17, the correction is obtained from the measured sheet resistances [see Tables I and III and Eq. (12)]. For point No. 18, the correction was chosen for the best results in this and in Fig. 12, since resistance measurements are not presently available for point No. 18. Data taken from Tables I–III, see Appendix.

materials and materials for which there are ambiguous parameters or insufficient data are represented as open circles. The open squares (numbers 19–26) correspond to non-high-T_c-like superconductors. The data for the optimal high-T_c materials exhibit obvious correlations that should not be ignored in any attempt to understand the high-T_c pairing mechanism. We shall return to a more detailed discussion of Figs. 10–13 after deriving the correlations (solid lines) one might expect on the basis of a simple Coulomb-coupling hypothesis.

INTERLAYER-COUPLING THEORIES

Studies[62] of $YBa_2Cu_3O_{7-\delta}/PrBa_2Cu_3O_{7-\delta}$ superlattices have shown that near-isolated pairs of CuO_2 planes exhibit superconductivity, although with a markedly lower and broader transition temperature than that of pure $YBa_2Cu_3O_{7-\delta}$. These studies conclude that while intercell coupling between pairs of CuO_2 sheets may enhance T_c, it is not necessary for superconductivity. Unfortunately, no study of a single CuO_2 layer exists, so the question of whether the coupling is interlayer or intralayer remains unanswered by these experiments. Nevertheless, the absence of coherence effects suggests that we should consider seriously the possibility of interlayer coupling. To set up a framework for evaluating the data in Table III, we shall use the relations among the parameters of a 2D system predicted by a simple interlayer Coulomb-coupling model. Based essentially on geometry, our interlayer-coupling model provides a way to look for correlations between several different types of measurements. Before presenting our model, however, we look very briefly at a sampling of related theories.

The present status of theories of high-T_c superconductivity is summarized for example by Abrahams,[63] in the

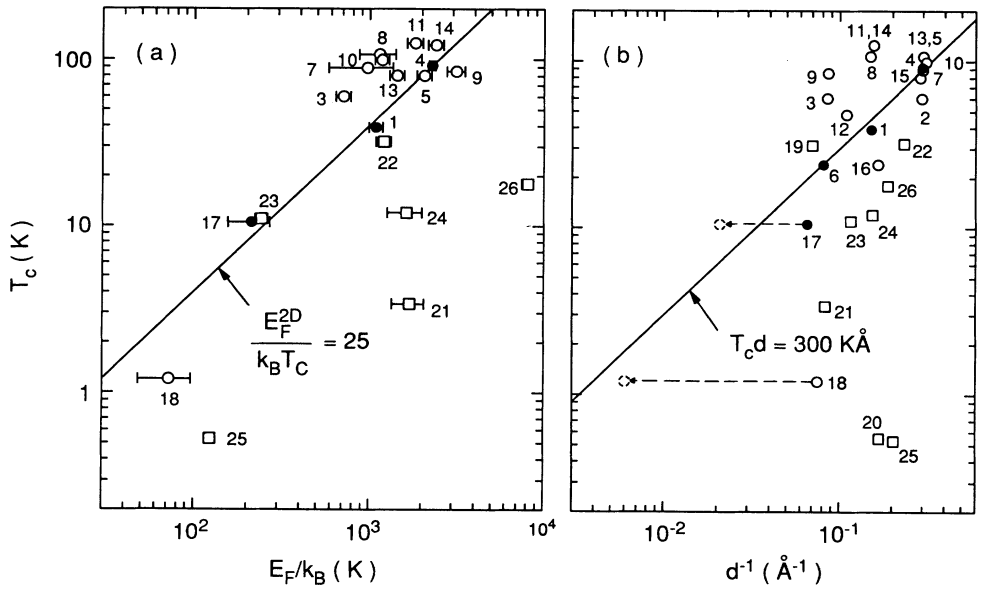

FIG. 12. The transition temperature, T_c vs the (a) 2D Fermi temperature, E_F/k_B, and (b) inverse of the interplanar spacing, d^{-1}. The solid circles represent data for materials having unambiguous geometries and that reasonable satisfy the criteria for sample phase-purity and minimum disorder effects. The lines correspond to Eq. (11) with the proportionality constants chosen to agree with point No. 4. The dashed lines and circles represent corrections for the average dielectric functions (see caption of Fig. 11). Point No. 5 in frame (a) corresponds to $HoBa_2Cu_4O_8$. Data taken from Tables I–III, see the Appendix.

book by Phillips,[64] and in various conference proceedings.[65] Tešanović[66] has considered an attractive interlayer Coulomb coupling that "may contain contributions from plasmon-, exciton-, and phonon-assisted transitions, as well as direct Coulomb interaction between charged layers," under the assumption that the direct hopping between layers is vanishingly small. Tešanović also asserts that the direct Coulomb coupling enhances the transition temperature regardless of its sign, and that a small hopping matrix element between layers reduces T_c. In another study, it was recently noted by Xiang *et al.*[67] that ". . . the CuO_2 sheets are the critical structural unit. Carrier doping in the sheets, and the strength of the coupling between adjacent (and possibly more distant) sheets, may to a large extent dictate the T_c for a given material." Xiang *et al.* conclude from their data on bismuth cuprates that the interplane hopping model proposed by Wheatly, Hsu, and Anderson[68] and the intraplane coupling model of Ihm and Yu,[69] might each have some merit in explaining the observed changes of T_c upon iodine intercalation.[67]

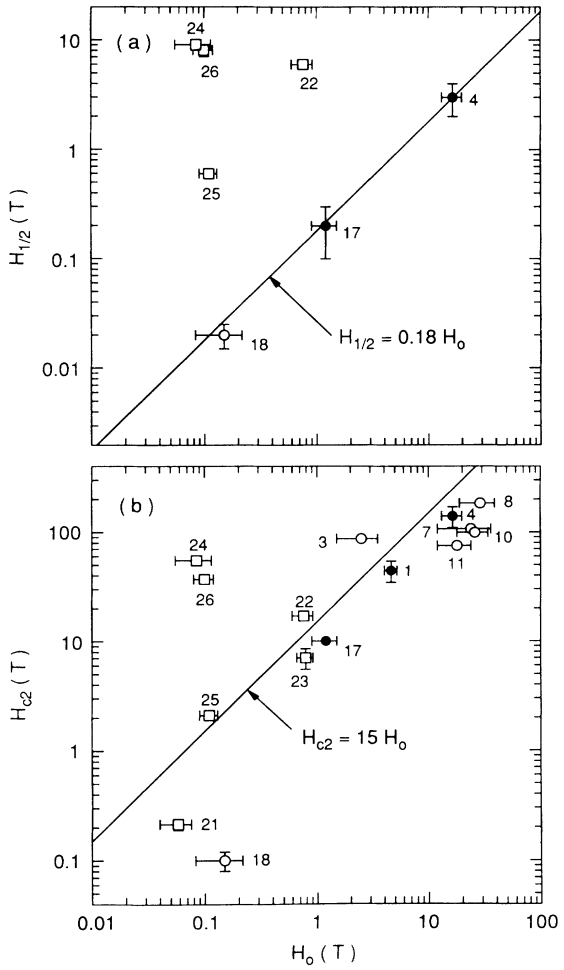

FIG. 13. The (a) field for half quenching the specific-heat jump, $H_{1/2}$, and (b) the upper critical field, H_{c2}, versus the characteristic field, H_0, defined in Eq. (17). The solid circles in both (a) and (b) represent data for materials having unambiguous geometries and that reasonably satisfy the criteria for sample phase-purity and minimum disorder effects. The line in frame (a) corresponds to Eq. (18) with the proportionality chosen to agree with point No. 4. Similarly the line shown in frame (b) corresponds to Eq. (19). Data taken from Tables I–III, see Appendix.

A number of other theories have also been proposed. Ye, Umezawa, and Teshima[70] have developed a model that includes "bridge pairing," by which is meant "a Cooper pair with one electron in one sheet and its partner in the nearest sheet. . . ." Unfortunately, they do not consider what it is that "mediates the pair interaction, although an interesting candidate for this is the surface phonon associated with the sheets." On the other hand, Lal and Joshi[71] present a model for screened Coulomb pairing but do not consider interlayer interactions. Another approach is the suggestion of Eschrig and Drechsler[72] that the pairing is due to "charge fluctuations between CuO_2 planes and the chains that are doping them." Kirkpatrick and Belitz[73] have a purely electronic mechanism for superconductivity in a disordered Fermi liquid that leads to triplet even-parity pairing in two dimensions, and so is not applicable to the high-T_c superconductors. Inoue *et al.*[74] have a model of interlayer Cooper pairing of two-dimensional electrons that are coupled through the exchange of three-dimensional phonons.

Other approaches include a theory in which the pairing state is represented phenomenologically by a local quantum field,[75] and an argument by Laughlin[76] that the elementary excitations of the Anderson resonating-valence-bond model[2] might obey fractional statistics and that a gas of such particles would form a qualitatively different kind of superconductor. On the other hand, Varma *et al.*[77] and Littlewood and Varma[78] have reduced the high-T_c problem to one of obtaining a certain momentum and frequency dependence of the charge and spin polarizability.[79]

MODEL FOR INTERLAYER COULOMB COUPLING

Many who believe that high-T_c Cooper pairing is attributable to Coulomb forces would agree that the key ingredient is the energy- and momentum-dependent dielectric function ϵ of the solid. According to Littlewood[80] simple exciton, plasmon, and charge fluctuation mechanisms are unlikely candidates for promoting superconductivity. Dayan[81] has presented a proof that spin-independent nonphononic mechanisms cannot provide an attractive pairing interaction between carriers at the phonon energy range without leading to crystal instability. However, he states that a nonphononic attractive interaction is possible at energies higher than the Debye energy. The recent model by Friedberg and Zhao[82] also suggests that dielectric screening can overcome the bare Coulomb repulsion in some cases, leaving a net attractive force between like charges.

In the interest of simplicity, we would like to consider as a working hypothesis the possibility of interlayer Coulomb pairing where the 2D carriers themselves provide the essential part of the dielectric function, while the rest of the solid provides an average dielectric back-

ground. If interlayer hopping is taken to be negligible in order to explain the absence of the Hebel-Slichter anomaly, there will be only one interaction length scale, the effective Bohr radius $a_0^* \equiv \hbar^2\epsilon/m_{ab}^* e^2$, where ϵ is an average dielectric constant, and m_{ab}^* is the 2D effective mass of the carriers. A pair of charge-carrying sheets is specified by three lengths: the separation d between the sheets, the inverse of the Fermi wave vector, k_F^{-1}, and the transverse confinement width w of one of the sheets. In our model, we would expect different systems having equal values for the three lengths when expressed in units of a_0^* to have equivalent electronic properties when expressed in units of the 2D Fermi energy. It follows that if we find a set of values d/a_0^*, $(a_0^* k_F)^{-1}$, and w/a_0^* that optimizes the superconducting properties of one system, the same set of values will be found for other optimally Coulomb-coupled layered superconductors. Evidence favoring our simple interlayer Coulomb-coupling hypothesis would thus be the presence of such constants in the available data.

For optimal coupling, we argue that the three lengths d, k_F^{-1}, and w should be roughly equal, while the dimensionless Wigner-Seitz radius [the average distance between carriers divided by the effective Bohr radius, i.e., $r_s \equiv \sqrt{2}(k_F a_0^*)^{-1}$] should have a value $r_s = r_s^0$, somewhat less than the $r_s \approx 37$ at which the Wigner crystal forms for a single-layer 2D electron gas.[83] A recent calculation by Świerkowski, Neilson, and Szymański[84] found that the tendency for Wigner crystallization[83,85] of a sheet of charge is enhanced by the proximity of a second sheet, and that as the interlayer spacing d decreases, the density at which crystallization occurs increases. The value of r_s favoring the Wigner crystal is between 10 and 20, and the layer spacing is roughly the same as the average distance between carriers. If r_s is less than 10, a charge-density wave results. The authors conclude "that the behavior of the system is critically dependent only on the planar electron density and the spacing between the layers, and not on the form of the single-particle distribution function $n(p)$, the layer thickness, or the number of layers." These results are particularly interesting in light of work by Küchenhoff and Schiller[86] showing "that the dilute electron gas [in 3D] is unstable against formation of Cooper pairs, the purely repulsive Coulomb interaction providing an attractive interaction . . . [due to] transverse current fluctuations." A transition temperature of 3 K is found for $r_s = 60$. Possibly T_c would increase if the carriers were confined to planar conducting sheets and if interplanar coupling were included. One possibility is that the normal modes of the Wigner lattice provide an attractive interaction between carriers in neighboring planes. In analogy with BCS theory, the Wigner crystal would then be unstable and a small fraction of the carriers would be paired below a critical temperature. From the results of Ref. 84, one condition for optimizing the pairing would be to have

$$n_{2D} d^2 = \beta_1 , \tag{9}$$

where β_1 is of order unity and weakly dependent on w/d. A requirement for there to be a significant interaction between particles in separate planes is thus to have the spacing between the charges in one plane match the distance between planes, i.e. $dk_F \approx \sqrt{2\pi}$.

It will also be necessary that the interplanar Coulomb interaction, $V_I = e^2/\epsilon d$, have the proper size relative to the 2D Fermi energy. If V_I is too large, the carriers in neighboring planes will behave as if they belonged to only a single plane; if V_I is too small, it will be too weak to yield an interplanar bound state. This condition is the same as requiring r_s to have its optimal value,[84] $r_s^0 \approx 15$, and combined with Eq. (9) may be written as

$$\frac{m_{ab}^* d}{\epsilon} = \sqrt{\pi\beta_1}\, r_s^0 m_e a_0 , \tag{10a}$$

or equivalently,

$$d = \sqrt{\pi\beta_1}\, r_s^0 a_0^* \equiv \beta_2 a_0^* . \tag{10b}$$

To reduce the repulsive intralayer Coulomb interactions, one would want w to be as large as possible without causing significant tunneling between sheets, that is $w \approx d$. However, r_s^0 is only weakly dependent on w/d according to Ref. 84.

In the BCS theory, T_c is given by[6]

$$k_B T_c = 1.14\hbar\omega_c (e^{1/\Lambda} - 1)^{-1} ,$$

where, Λ $[= N(0)V]$ is the BCS coupling constant, and in our 2D case, $N(0) = 1/E_F^{2D}$ is the density of states (per unit area) at the Fermi surface. If we assume $\hbar\omega_c \approx E_F^{2D}$, then we find $\Lambda \approx 0.3$ for the high-T_c superconductors, corresponding to weak coupling. While small variations in Λ only weakly affect the effective-mass values extracted from $\Delta C/T_c$, their influence could be substantially enhanced when placed in the exponential. If the BCS interaction V is some fraction of V_I and the cutoff energy of the excitation spectrum $\hbar\omega_c$ is proportional to the 2D Fermi energy E_F^{2D}, we then have

$$k_B T_c = \beta_3 E_F^{2D} , \tag{11a}$$

and making use of Eqs. (9) and (10),

$$k_B T_c = \frac{2\sqrt{\pi\beta_1}\, R_\infty \beta_3 a_0}{r_s^0 \epsilon d} \propto (\epsilon d)^{-1} . \tag{11b}$$

Equation (11a) is a statement that there is only one energy scale in the problem, which is to say that we are ignoring the energy dependence of the dielectric function ϵ. Given the restriction to the conditions of optimal superconductivity, β_3 should have a similar value for various systems, although its dependence on w/d and the nonconstancy of ϵ could be more significant than that of β_1 due to the exponential factor appearing in the BCS formula.

A further electronic property that we may consider is the sheet resistance of a single layer $R(T) = \rho(T)/\delta$, where $\rho(T)$ is the resistivity and δ is the average spacing between layers. If the linearity of the normal-state resistivity is an intrinsic high-T_c property ascribable to Coulomb interactions alone, then we expect that the sheet resistance at a characteristic temperature such as

T_c will be proportional to the inverse of a characteristic velocity such as the Fermi velocity v_F. Given the restriction to optimal superconductivity, Eqs. (9) and (10) then imply that the sheet resistance at T_c is proportional to $\epsilon h/e^2=\epsilon R_K$, where R_K is again the von Klitzing quantum-Hall-effect resistance.[58] Thus, we expect

$$R(T_c)=\beta_4 R_K \epsilon , \tag{12}$$

where we might speculate that $\beta_4 \approx 1/r_s^0$. In general, the resistivity is given by

$$\rho(T)=4\pi\omega_p^{-2}\tau^{-1} , \tag{13}$$

where the scattering rate in the model of Littlewood and Varma[78] is $\tau^{-1}\approx k_B T/\hbar$,[77,87] where the plasma frequency in a background dielectric is

$$\omega_p^2=4\pi n_{3D}\frac{e^2}{m^*\epsilon} . \tag{14}$$

For a layered system, the plasma frequency is still given by Eq. (14) for plasma wave vectors parallel to the conducting planes,[88] and becomes

$$\omega_p^2=\frac{4\pi n_{2D}e^2}{m_{ab}^*\delta\epsilon}=4E_F^{2D}\frac{e^2}{\hbar^2\delta\epsilon} . \tag{15}$$

In principle one should be able to obtain the 2D Fermi energy from the plasma energy, $E_F^{2D}=E_p^2\epsilon\delta/4e^2$, where $E_p\equiv\hbar\omega_p$. In this model, the sheet resistance at the transition temperature becomes

$$R(T_c)=\frac{1}{2}\epsilon R_K\frac{k_B T_c}{E_F^{2D}} , \tag{16}$$

which is very similar to Eq. (12), and in fact gives a good approximation to the measured sheet resistance. One possible conclusion would be that our working hypothesis is not in conflict with the polarizability posited in the model of Varma *et al.*[77]

If the rate of decrease of the specific-heat jump at T_c, $\Delta C/T_c$, with increasing magnetic field is another intrinsically high-T_c property, then the field $H_{1/2}$ that reduces $\Delta C/T_c$ to half its zero-field value should be proportional to a magnetic field characteristic of the Coulomb-coupled sheets. One such characteristic field H_0 is the field at which there is a single flux quantum ϕ_0 enclosed within a circle of radius equal to a characteristic length such as $b=\hbar v_F/k_B T_c$ (the Pippard coherence length is given by $\xi_0=a\hbar v_F/k_B T_c$, where $a=(1.76\pi)^{-1}=0.18$ in the BCS theory):

$$H_0=\frac{\phi_0}{\pi b^2}=\frac{\phi_0}{2\pi}\hbar^{-2}m^*k_B^2T_c^2(E_F)^{-1}$$

$$=0.3725\frac{m^*}{m_e}\frac{T_c^2}{E_F k_B^{-1}}\ \text{(T)} , \tag{17}$$

for T_c given in K, and where m^* and E_F are the appropriate two- or three-dimensional quantities. We would then expect to find

$$H_{1/2}=\beta_5 H_0 . \tag{18}$$

The possibility of interlayer coupling could be further studied using the field dependence of the fluctuation correlation length, which is directly reflected in the field-dependence of $\Delta C/T_c$.[38,39] On the basis of the Ginzberg-Landau theory,[89] the upper critical field H_{c2} is expected to satisfy the relation

$$H_{c2}=H_0/2a^2\approx 15H_0 . \tag{19}$$

The same theory also relates the lower critical field H_{c1} and the critical current to H_{c2}; one would expect the Ginzberg-Landau parameters for optimal Coulomb-coupled superconductors to be similar. For the high-T_c materials, Eqs. (17–19) provide an alternate way of estimating H_{c2}. The field at which the $n=1$ quantized Hall resistance plateau would appear for an isolated conducting plane would be $H_1=4(E_F^{2D}/k_B T_c)^2H_0=4\beta_3^{-2}H_0$ $\approx 2500H_0$. Finally, it is interesting that our hypothesis implies that the coefficient of the $1/f$ noise[90] and magnetoresistance[91] will also satisfy correlations with the other electronic parameters.

DISCUSSION

We now return to our discussion of Figs. 10–13. Figure 10(a) shows the 2D carrier density n_{2D} versus the inverse square of the interlayer spacing, d^{-2}. The line corresponds to Eq. (9) with $\beta_1=1$. Points not falling on the line $n_{2D}d^2=1$ correspond to either non-high-T_c-like superconductors or high-T_c-like samples presenting less than optimal characteristics from the materials or measurement perspective, and which are therefore expected to show suppressed effective n_{2D} values. While the correlation exhibited by the layered high-T_c-like materials (circles) is clear, there are exceptions. Specifically, we note that n_{2D} for $Tl_2Ba_2CaCu_2O_8$ (point No. 10) falls short of the expected value, assuming $d\approx 3.2$ Å. As noted in the Appendix, however, the $\Delta C/T_c$ value quoted is a lower-limit since $\rho(T>T_c)$ for the sample measured exhibits serious deviations from the expected $\propto T$ behavior. The fact that n_{2D} for $YBa_2Cu_4O_8$ (point No. 5) also appears too small is not surprising given the small Meissner fractions resported, and the apparent peak in T_c at elevated pressures, indicating that this material may not be optimum at ambient pressure. The data for $(Tl_{0.5}Pb_{0.5})(Sr_{2-x}La_x)(Ca_{1-y}Y_y)CuO_7$ (point No. 13) also show a 2D carrier density too small for the assigned interlayer spacing. However, as pointed out in the Appendix, this material has a peak T_c of 107 K and $\rho(0)$ only approaches zero for $x=0.2$. Unfortunately, $\lambda_{ab}(0)$ and $\Delta C/T_c$ were measured on a sample with $x=0$, with the latter increasing by almost a factor of 2 from $x=0$ to $x=0.2$. Thus, point No. 13 as plotted corresponds to measurements made on nonoptimized samples. Since $\rho(T>T_c)$ is slightly nonlinear, it is tempting to characterize $YBa_2Cu_3O_{6.67}$ (point No. 3) as a nonoptimized version of $YBa_2Cu_3O_7$ (point No. 4). However, because $YBa_2Cu_3O_{6.67}$ also exhibits a full Meissner fraction, we assume the pairing to be between the CuO_2 double layers. While contributions from the chains could be also significant as discussed above, we are unable to account

for them at this time. Owing to flux-lattice dynamics and longitudinal disorder effects found in $Bi_2Sr_2CaCu_2O_8$ (point No. 7), we have been unable to reliably establish $\lambda_{ab}(0)$. Specific-heat measurements at T_c also appear to be rather unreliable, as evidenced by the wide range of sample-dependent variations.

While several researchers have looked for chemical trends to explain high-T_c superconductivity,[64,92,93] it would seem unlikely that the correlation shown in Fig. 10(a) could be of chemical origin, (e.g., one carrier per atom, etc.) given that the organic superconductor, κ-[BEDT-TTF]$_2$Cu[NCS]$_2$ (point No. 17), is of such different chemistry and geometry from the cuprates. As shown in Fig. 9, a maximum occurs in T_c as the number of carriers is changed by doping.[17] The fact that the maximum occurs for $n_{2D}d^2 \approx 1$ is in accord with the concept behind Eq. (9). Further evidence against a chemical origin of $n_{2D}d^2=1$ is the lack of correlation between n_{2D} and the inverse of the basal-plane area per formula unit, as shown in Fig. 10(b).

Batlogg *et al.*[94] have collected a number of γ values for phase-pure superconductors representative of most of the known superconducting families, but find no clear evidence of a relationship between T_c and γ. According to Eq. (4), m_{ab}^*/m_e is directly related to γ, and by Eq. (10) would be proportional to ϵ/d if there is any validity to our simple hypothesis. The effective mass m^*/m_e is plotted against the inverse interplanar distance d^{-1} in Fig. 11. The datum for κ-[BEDT-TTF]$_2$Cu[NCS]$_2$ (point No. 17) can be brought in line (dashed circle) with that of high-T_c cuprates by dividing its m_{ab}^*/m_e value by the ratio of its sheet resistance to that of $YBa_2Cu_3O_7$ [see Eq. (10a)], an operation that should correct for the different average dielectric functions according to Eq. (12). A similar operation might work for [TMTSF]$_2$ClO$_4$ (point No. 18). The dashed line shows where point No. 18 might be if we correct for the difference in the average dielectric constant from point No. 4 in such a way as to agree with Fig. 12(b) as discussed below. The effective masses for both $YBa_2Cu_4O_8$ (point No. 5, $T_c=80$ K) and $(Tl_{0.5}Pb_{0.5})Sr_2CaCu_2O_7$ (point No. 13, $T_c=80$ K) are markedly low in comparison to the line. Since neither of these materials possess the maximum T_c of their respective groups, the apparent suppression in m_{ab}^* is consistent with these materials not being optimum. Assuming that the relevant average dielectric constant for the cuprates is the high-frequency $YBa_2Cu_3O_7$ value,[95] $\epsilon=4.0\pm0.5$, the data suggest $\beta_2 \approx 15$ and therefore $r_s^0 \approx 9$. However, since we do not accurately know the dielectric function, the r_s^0 value appropriate for superconductivity is not well determined. The $R=(685\pm85)$ Ω sheet resistance for $YBa_2Cu_3O_7$ implies $\beta_4^{-1} \approx 140$. The basal-plane resistivity $\rho(T)$ has also been examined by Batlogg,[96] but no functional dependence of T_c on the slope $d\rho/dT$ was found. However, in light of Eq. (12) one might actually expect $d\rho/dT \propto \epsilon\delta/T_c$ for materials having $\rho(0)=0$.

Figure 12(a) shows T_c versus E_F/k_B, where E_F represents the appropriate 2D or 3D value defined in Eq. (5). The points representing the optimized materials having unambiguous measured parameters (filled circles) suggest $\beta_3^{-1} \approx 25$. Both $Bi_2Sr_2CaCu_2O_8$ (point No. 7), and $Tl_2Ba_2CaCu_2O_8$ (point No. 10) fall well short of the line, which from Eq. (5) suggests that either the measured values of $\lambda_{ab}(0)$ are too great or perhaps the BiO_2/TlO_2 layers are superconducting. Point No. 13, $(Tl_{0.5}Pb_{0.5})Sr_2CaCu_2O_7$ ($T_c=80$ K), also shows a departure from the line, which as we have already discussed is possibly attributable to the material being nonoptimal. Since for $YBa_2Cu_3O_{6.67}$ (point No. 3) we assume pairing between double CuO_2 layers, the relevant energy scale might be twice that of a single sheet, which would place the point on the line indicated in Fig. 12(a). In fact, the relevant parameter might be the density of states at the Fermi level, which is equal to $2E_F^{2D}$ for the double-layer pairing scheme assumed for $YBa_2Cu_3O_{6.67}$.

Several previous studies[19,51,92,93,97] have been conducted with the intent of finding correlations between T_c and other electronic properties related to E_F. While many of these studies presented interesting correlations, information about the superconducting state was clouded by disorder effects associated with continuous doping of the high-T_c cuprates and neglect of variations in the effective mass m_{ab}^* and the average plane spacing δ. For example, one could imagine comparing T_c to the μ^+SR linewidth, $\sqrt{\langle(\Delta B)^2\rangle}$, which is related to $\lambda_{ab}^{\rm eff}(0)$ via Eq. (7). As discussed above in connection with Fig. 8, this approach yields data exhibiting a linear dependence of T_c with $(\lambda_{ab}^{\rm eff})^{-2}$, which is not intrinsic to high-T_c superconductivity but rather due to disorder effects, and may explain the simultaneous disappearance of the isotope effect and the residual resistivity at optimal doping.

In Figure 12(b) we plot T_c versus d^{-1}. While these two quantities are relatively free of measurement errors associated with the penetration depth and specific heat, T_c is always a lower limit, and the correct value of d is not always unambiguous. Indeed, the interlayer spacings d for $(Bi_{1.6}Pb_{0.4})Sr_2Ca_2Cu_3O_{10}$ (point No. 8), $Tl_2Ba_2Ca_2Cu_3O_{10}$ (point No. 11), and $(Tl_{0.5}Pb_{0.5})Sr_2Ca_2Cu_3O_9$ (point No. 14) may actually be ~ 3.2 Å rather than the ~ 6.4 Å we have assumed. If interpreted within the context of our interlayer coupling model, departures from the line of $T_c d=300$ K Å might simply be reflecting variations in ϵ. Both κ-[BEDT-TTF]$_2$Cu[NCS]$_2$ (point No. 17) and [TMTSF]$_2$ClO$_4$ (point No. 18) can be brought into line with the high-T_c cuprates by using the same average dielectric constants [see Eq. (11b)] that shift these data points close to the line in Fig. 11. We note again that the ratio, ϵ(No. 17)/ϵ(No. 4), is taken to be the measured ratio of the respective sheet resistances, as expected from Eq. (12).

Finally, based on Eqs. (18) and (19), we have plotted $H_{1/2}$ and H_{c2} against H_0 in Figs. 13(a) and 13(b) respectively. Unfortunately, we have values for both $H_{1/2}$ and H_0 for only a few materials, making this comparison somewhat incomplete. Nevertheless, the data in frame (a) for $YBa_2Cu_3O_7$ (point No. 4), κ-[BEDT-TTF]$_2$Cu[NCS]$_2$ (point No. 17), and [TMTSF]$_2$ClO$_4$ (point No. 18) suggest $\beta_5^{-1} \approx 5.5$. The data for [TMTSF]$_2$ClO$_4$ were obtained with $\mathbf{H}_{\rm ext}$ oriented along the c axis. The effective mass

along the a axis m_a^* was derived directly from $\Delta C/T_c$ measurements, and was combined with transfer integral calculations to estimate m_b^*; m_{ab}^* was then obtained assuming the geometric average, $m_{ab}^*=\sqrt{m_a^* m_b^*}$. Although the H_{c2} data are relatively unreliable, the correlation of H_{c2} with H_0 for the high-T_c materials agrees roughly with Eq. (19). In particular, the value of H_{c2} shown in frame (b) for $[TMTSF]_2ClO_4$ (point No. 18) is taken from data extending only down to ~ 0.5 K, leaving open the possibility that H_{c2} is actually greater than that shown (see, e.g., analogous measurements on κ-[BEDT-TTF]$_2$Cu[NCS]$_2$ which show an upturn in dH_{c2}/dT below ~ 2 K).

CONCLUSION

The suppression of both isotope and coherence effects, the apparent s-wave ground state, and the unique normal-state properties found in the layered cuprate superconductors have led us to consider the possibility of Cooper pairing due to the interlayer Coulomb coupling of confined carriers, and the concomitant importance of the interlayer spacing d. Given the 2D character of the high-T_c cuprates, we also assume the intrinsic importance of the 2D carrier density n_{2D}, effective mass m^*, 2D Fermi energy, E_F^{2D}, and sheet resistance of a single conducting plane $R(T_c)$. We have tabulated the relevant data available on a range of high-T_c cuprates and other superconductors, and determined those properties intrinsic to high-T_c superconductivity. Guided in part by our assumption of Coulomb mediation, we have searched for correlations between the various parameters. Although partially limited by the quality of existing data, we find that phase-pure layered compounds of optimized composition (i.e., stoichiometry optimized for highest T_c, near zero residual resistivity, etc.) exhibit correlations of the form $n_{2D}d^2=1$, $m^*\propto\epsilon/d$, $k_BT_c\propto 1/\epsilon d\propto E_F^{2D}$ and $H_{1/2}\propto H_0$. We interpret these correlations in terms of a simple model expressed in Eqs. (9)–(12) and (17), providing evidence that several important structural and electronic parameters of the superconducting state are correlated in a manner consistent with our hypothesis of interlayer Coulomb coupling. If the latter is incorrect, then one must still note that the closely coupled conducting planes of the layered superconductors happen to satisfy the conditions for exhibiting strong Coulomb correlation effects.

Unfortunately, the data available at present are not of sufficient quality to establish definitively the validity of our Coulomb-pairing hypothesis, and further investigation on this matter would be justified. Specifically, we require a set of careful measurements of all quantities of interest performed on the same single-crystal samples optimized for the highest T_c and minimal disorder effects. An alternate approach that might provide a definitive test would be to study "high-T_c"-like layered structures made from various materials such as graphite-boron nitride layers,[98] organometallic sandwich polymers,[99] or quantum well $Ga_{1-x}Al_xAs$ heterostructures.[100]

ACKNOWLEDGMENTS

We are grateful to L. R. Monar for his help in compiling the information in Tables I and II. We also thank B. Batlogg, W. F. Brinkman, A. T. Fiory, P. A. Fleury, R. C. Haddon, P. B. Littlewood, C. A. Murray, L. N. Pfeiffer, P. M. Platzman, T. T. M. Palstra, A. P. Ramirez, M. A. Schlüter, R. E. Slusher, and G. A. Thomas for helpful discussions.

[1] J. G. Bednorz and K. A. Müller, Z. Phys. B **64**, 188 (1986).
[2] P. W. Anderson, Science **235**, 1196 (1987). For recent discussions see T. W. Barbee III, M. L. Cohen, and D. R. Penn, Phys. Rev. B **44**, 4473 (1991); Ju H. Kim, K. Levin, R. Wentzcovitch, and A. Auerbach, *ibid.* **44**, 5148 (1991).
[3] L. N. Cooper, Phys. Rev. **104**, 1189 (1956).
[4] L. C. Hebel and C. P. Slichter, Phys. Rev. **113**, 1504 (1959).
[5] C. E. Gough, M. S. Colclough, E. M. Forgan, R. G. Jordan, M. Keene, C. M. Muirhead, A. I. M. Rae, N. Thomas, J. S. Abell, and S. Sutton, Nature **326**, 855 (1987).
[6] J. Bardeen, L. N. Cooper, and J. R. Schrieffer, Phys. Rev. **108**, 1175 (1957).
[7] D. R. Harshman *et al.*, Phys. Rev. B **36**, 2386 (1987).
[8] D. Mandrus *et al.*, Phys. Rev. B **44**, 2418 (1991).
[9] J. C. Phillips, Phys. Rev. Lett. **64**, 1605 (1990).
[10] K. A. Müller, Z. Phys. B **80**, 193 (1990).
[11] T. Koyama and M. Tachiki, Phys. Rev. B **39**, 2279 (1989).
[12] Based on experience with $La_{1.85}Sr_{0.15}CuO_4$, it is probable that titration measurements can be reasonably accurate for simple optimized structures that would also include $(Bi,Tl)_2(Sr,Ba)_2CuO_6$.
[13] A. B. Pippard, Proc. R. Soc. London **A216**, 547 (1953); P. G. de Gennes, *Superconductivity of Metals and Alloys* (Benjamin, New York, 1966), p. 25. Note that we consider only the limit where $l \ll \lambda_L(0)$.
[14] D. R. Harshman *et al.*, Phys. Rev. B **39**, 851 (1989).
[15] C.-K. Loong *et al.*, Phys. Rev. Lett. **66**, 3217 (1991). See also A. I. Liechtenstein *et al.*, Phys. Rev. B **44**, 5388 (1991).
[16] C.-C. Chen and C. M. Lieber, J. Am. Chem. Soc. (to be published), obtain $\alpha=0.3\pm0.06$ for K_3C_{60}; A. P. Ramirez *et al.*, Phys. Rev. Lett. **68**, 1058 (1992), find $\alpha=0.38\pm0.05$ for Rb_3C_{60}.
[17] M. K. Crawford *et al.*, Phys. Rev. B **41**, 282 (1990); C. C. Tsuei *et al.*, Phys. Rev. Lett. **65**, 2724 (1990).
[18] J. P. Franck *et al.*, Physica B **169**, 697 (1991); J. P. Franck *et al.*, Phys. Rev. B **44**, 5318 (1991), isotope effect in $(Y_{1-x}Pr_x)Ba_2Cu_3O_z$; J. C. Phillips, *ibid.* **43**, 6257 (1991); H. J. Bornemann and D. E. Morris, *ibid.* **44**, 5322 (1991), isotope effect in $YBa_{2-x}La_xCu_3O_z$.
[19] S. S. Laderman *et al.*, Phys. Rev. B **43**, 2922 (1991), normal-state resistivity in $YBa_2Cu_3O_{7-\delta}$; A. Podder, *et al.*, *ibid.* **44**, 2757 (1991); see also Ref. 8, resistivity measurements on $Bi_2Sr_2(Ca_{1-x}Y_x)Cu_2O_8$.
[20] M. Gurvitch and A. T. Fiory, Phys. Rev. Lett. **59**, 1337 (1988).
[21] K. Bechaard *et al.*, Phys. Rev. Lett. **46**, 852 (1981).
[22] R. J. Cava *et al.*, Nature **329**, 423 (1987); Physica C **165**, 419

(1990).
[23]S. Martin *et al.*, Phys. Rev. B **39**, 9611 (1989).
[24]T. T. M. Palstra *et al.*, Phys. Rev. Lett. **68**, 1054 (1992), present measurements on thin films that suggest the Pippard (clean-limit) coherence length in the absence of granularity to be in the range $100 \lesssim \xi_0 \lesssim 200$ Å.
[25]K. Semba *et al.*, Phys. Rev. Lett. **67**, 769 (1991).
[26]A. Ugawa *et al.*, Synth. Met. **27**, A445 (1988).
[27]P. H. Hor *et al.*, Phys. Rev. Lett. **58**, 911 (1987); A. Driessen *et al.*, Phys. Rev. B **36**, 5602 (1987).
[28]B. P. Singh *et al.*, J. Mater. Sci. **25**, 4630 (1990); R. J. Wijngaarden *et al.*, Physica C **152**, 140 (1988).
[29]K. Murata *et al.*, Synth. Met. **27**, A341 (1988).
[30]R. J. Wijngaarden *et al.* (unpublished).
[31]B. Batlogg (private communication) assumes a factor of five; T-K. Xia and D. Stroud, Phys. Rev. B **37**, 118 (1988), shows a theoretical factor of two.
[32]R. Tycko *et al.*, Phys. Rev. Lett. **68**, 1912 (1992), present data indicating the absence of a Hebel-Slichter peak in K_3C_{60}.
[33]M. C. Nuss, P. M. Mankiewich, M. L. O'Malley, E. H. Westerwick, and P. B. Littlewood, Phys. Rev. Lett. **66**, 3305 (1991); K. Holczer *et al.*, *ibid.* **67**, 152 (1991), have reported similar data on $Bi_2Sr_2CaCu_2O_8$, but incorrectly interpret the peak in the conductivity as evidence for case-II coherence factors.
[34]P. C. Hammel *et al.*, Phys. Rev. Lett. **63**, 1992 (1989).
[35]T. Takahashi *et al.*, Synth. Met. **27**, A319 (1988); D. Schweitzer *et al.*, *ibid.* **27**, A465 (1988).
[36]R. E. Walstedt (private communication); F. Creuzet *et al.*, Physica B **143**, 363 (1986), also report a peak in $1/T_1$ for β-[BEDT-TTF]$_2$I$_3$ just below T_c, which like the 10 K Cu[NCS]$_2$ material is field dependent and not associated with coherence factor effects; D. R. Harshman *et al.* (unpublished), present results suggesting that the peak in $1/T_1$ may be associated with a flux-pinning transition.
[37]D. Poilblanc *et al.*, Phys. Rev. Lett. **58**, 270 (1987), estimate transfer integral ratios for $t_a:t_b:t_c$ of 300:30:1. We obtain m_a^* from $\Delta C/T_c$. We estimate the effective mass in the b direction by noting that m_i^* is proportional to the inverse square of the transfer integral, t_i^{-2}. The 2D effective mass, m_{ab}^*, was then obtained assuming the geometric average, $m_{ab}^* = \sqrt{m_a^* m_b^*}$.
[38]S. E. Inderhees *et al.*, Phys. Rev. Lett. **60**, 1178 (1988); D. M. Ginsberg *et al.*, Physica C **153-155**, 1082 (1988); V. G. Zarifis and D. H. Douglass, *ibid.* **170**, 46 (1990); for 2D systems, the field dependence of the fluctuation contribution to $\Delta C/T_c$ is proportional to $\xi^2(T)/w$, where $\xi^2(T)$ is the Ginzberg-Landau coherence length and w is the thickness of the superconducting sheet. If the quasiparticles are paired between layers, however, then perhaps $w=d$. See, e.g., M. Tinkham, *Introduction to Superconductivity* (Kreiger, New York, 1980), Chap. 7.
[39]See, e.g., N. E. Phillips *et al.*, J. Appl. Phys. Jpn. Suppl. **26-3**, 1115 (1987); E. Boujour *et al.*, Physica B **165&166**, 1343 (1990); M. B. Salamon *et al.*, Phys. Rev. B **38**, 885 (1988).
[40]See, e.g., L. C. Brunel *et al.*, Phys. Rev. Lett. **66**, 1346 (1991); other experiments suggest deviations from conventional BCS weak-coupling.
[41]J. E. Graebner *et al.*, Phys. Rev. B **41**, 4808 (1990).
[42]P. Garoche *et al.*, Phys. Rev. Lett. **49**, 1346 (1982). These authors have also studied the effect of cooling rate on the detailed shape of $\Delta C/T_c$.
[43]W. Barford and J. M. F. Gunn, Physica C **156**, 515 (1988); A. Baratoff *et al.* (private communication) have also considered flux lattices where the field is not necessarily perpendicular to the basal plane.
[44]G. Aeppli *et al.*, Phys. Rev. B **35**, 7129 (1987); W. J. Kossler *et al.*, *ibid.* **35**, 7133 (1987); F. N. Gygax *et al.*, Europhys. Lett. **4**, 473 (1987); P. Birrer *et al.*, Physica C **158**, 230 (1989).
[45]E. H. Brandt, Phys. Rev. B **37**, 2349 (1988); E. H. Brandt and A. Seeger, Adv. Phys. **35**, 189 (1986).
[46]D. R. Harshman *et al.*, Phys. Rev. Lett. **64**, 1293 (1990).
[47]D. R. Harshman *et al.*, Phys. Rev. Lett. **67**, 3152 (1991); M. Inui and D. R. Harshman (unpublished).
[48]D. R. Harshman, A. T. Fiory, and R. J. Cava, Phys. Rev. Lett. **66**, 3313 (1991).
[49]D. R. Harshman *et al.*, Phys. Rev. Lett. **63**, 1187 (1989).
[50]Y. J. Uemura *et al.*, Phys. Rev. B **38**, 909 (1988), show a strong departure of $\lambda_{ab}(T)$ from the expected s-wave behavior for the "nominally" 60 K phase $YBa_2Cu_3O_{7-\delta}$, indicative of phase inhomogeneity. Harshman *et al.* (Ref. 14) indicate that this material is indeed s wave in nature, with a basal-plane penetration depth of $\lambda_{ab}(0)=2550\pm125$ Å.
[51]Y. J. Uemura *et al.*, Phys. Rev. Lett. **62** 2317 (1989). However, from Table I and Figs. 1 and 2, it is evident that ΔT_c, α, and/or $\rho(0)$ may increase with increased doping for most of the materials considered; C. L. Seaman *et al.*, Phys. Rev. B **42**, 6801 (1990), in a study of $(Y_{1-x}Pr_x)Ba_2Cu_3O_7$, use the small change in ΔT_c with doping to argue that one can continuously dope in this manner without altering the quality of the superconducting material. Unfortunately, the small variation in ΔT_c reported only shows that these materials are homogeneously disordered, while the effects of disorder are clearly reflected in $\rho(0)$, α, and $\lambda(0)$ (see Table I and Figs. 1, 2, and 8). Given these complications, one cannot conclude from these measurements that $T_c \propto E_F$.
[52]H. Urayama *et al.*, Chem. Lett. p. 55 (1988); G. Saito *et al.*, Synth. Met. **27**, A331 (1988).
[53]G. Rindorf *et al.*, Acta Crystallogr. **38**, 2805 (1982).
[54]M. A. Schlüter (private communication).
[55]M. Di Stasio, K. A. Müller, and L. Papietronoro, Phys. Rev. Lett. **64**, 2827 (1990).
[56]A. Trokiner *et al.*, Phys. Rev. B **44**, 2426 (1991); these authors refer also to unpublished band-structure calculations by R. J. Gupta, which apparently assigns 31% of the holes to the center layer.
[57]D. R. Harshman, R. N. Kleiman, and A. T. Fiory (unpublished).
[58]K. von Klitzing, Rev. Mod. Phys. **58**, 519 (1986).
[59]R. M. Fleming *et al.*, Nature **352**, 787 (1991).
[60]Y. J. Uemura *et al.*, Nature **352**, 605 (1991), have recently reported a μ^+SR measurement of $\lambda(0)\approx4800$ Å. Owing to an unknown effective mass, and possible finite-l corrections, however, it would be difficult to derive values for E_F or n_{3D}. Further measurements characterizing the sample qualtiy, i.e., resistivity (or rf-resistive loss), susceptibility, and specific heat would be necessary for a complete and accurate evaluation of this material. Recent band-structure calculations by S. C. Erwin and W. E. Pickett, Science **254**, 842 (1991), suggest a clean-limit value of $\lambda(0)=1600$ Å.
[61]A. Ramirez *et al.* (unpublished).
[62]D. H. Lowndes *et al.* Phys. Rev. Lett. **65**, 1160 (1990); Q. Li *et al.*, *ibid.* **64**, 3086 (1990); J.-M. Triscone *et al.*, *ibid.* **64**, 804 (1990); T. Terashima *et al.*, *ibid.* **67**, 1362 (1991).
[63]E. Abrahams, in *Advances in Superconductivity II,* edited by T. Ishiguro and K. Kajimura (Springer-Verlag, Tokyo, 1990), p. 7.
[64]J. C. Phillips, *Physics of High T_c Superconductors* (AT&T Bell

Laboratories and Academic, Boston, 1989).
[65]See various articles in *Towards the Theoretical Understanding of High T_c Superconductors,* edited by S. Lundqvist, E. Tosatti, M. P. Tosi, and Yu Lu (World Scientific, Singapore, 1988).
[66]Zlatko Tešanović, Phys. Rev. B **36**, 2364 (1987).
[67]X.-D. Xiang, A. Zetti, W. A. Vareka, J. L. Corkill, T. W. Barbee III, and M. L. Cohen, Phys. Rev. B **43**, 11 496 (1991). Subsequently, X.-D. Xiang *et al.*, Phys. Rev. Lett. **68**, 530 (1992), found that T_c is only slightly suppressed by iodine intercalation in $Bi_2Sr_2CaCu_2O_{8+\delta}$.
[68]J. M. Wheatley, T. C. Hsu, and P. W. Anderson, Nature (London) **333**, 121 (1988); P. W. Anderson, G. Baskaran, Z. Zou, and T. Hsu, Phys. Rev. Lett. **58**, 2790 (1987).
[69]J. Ihm and B. D. Yu, Phys. Rev. B **39**, 4760 (1989).
[70]Z. Ye, H. Umezawa, and R. Teshima, Phys. Rev. B **44**, 351 (1991).
[71]R. Lal and S. K. Joshi, Phys. Rev. B **43**, 6155 (1991).
[72]H. Eschrig and S.-L. Drechsler, Physica C **173**, 80 (1991).
[73]T. R. Kirkpatrick and D. Belitz, Phys. Rev. Lett. **66**, 1533 (1991).
[74]M. Inoue *et al.* (unpublished).
[75]R. Friedberg, T. D. Lee, and H. C. Ren, Phys. Lett. A **152**, 417 (1991); R. Friedberg and T. D. Lee, *ibid.* **152**, 423 (1991).
[76]R. B. Laughlin, Science **242**, 525 (1988); R. B. Laughlin, Phys. Rev. Lett. **60**, 2677 (1988).
[77]C. M. Varma *et al.*, Phys. Rev. Lett. **63**, 1996 (1989).
[78]P. B. Littlewood and C. M. Varma, J. Appl. Phys. **69**, 4979 (1991).
[79]B. R. Alascio and C. R. Proetto, Solid State Commun. **75**, 217 (1990).
[80]P. B. Littlewood, Physica B **163**, 299 (1990).
[81]M. Dayan, Solid State Commun. **67**, 1073 (1988).
[82]R. Friedberg and H. S. Zhao, Phys. Rev. B **44**, 2297 (1991).
[83]B. Tanatar and D. M. Ceperley, Phys. Rev. B **39**, 5005 (1989).
[84]L. Świerkowski, D. Neilson, and J. Szymański, Phys. Rev. Lett. **67**, 240 (1991).
[85]D. Nguyen Manh (unpublished).
[86]S. Küchenhoff and S. Schiller, Physica B **165&166**, 1033 (1990).
[87]P. B. Littlewood (private communication).
[88]D. Grecu, Phys. Rev. B **8**, 1958 (1973).
[89]V. L. Ginzberg and L. D. Landau, Zh. Eksp. Theor. Fiz. **20**, 1064 (1950).
[90]A. Maeda *et al.*, in Proceedings of the M^2S HTSC III Conference, Kanazawa, Japan, 1991 [Physica C **185-189**, 1301 (1991)].
[91]For recent references, see, e.g., T. W. Jing *et al.*, Phys. Rev. Lett. **67**, 761 (1991); see, also, Ref. 25.
[92]Y. Ohta, T. Ohyama, and S. Maekawa, Physica B **165&166**, 983 (1990).
[93]Y. Tokura *et al.*, Phys. Rev. B **38**, 7156 (1988).
[94]B. Batlogg *et al.*, IBM J. Res. Dev. **33**, 208 (1989).
[95]G. A. Thomas, in *Proceedings of the 39th Scottish Universities Summer School of Physics of High-Temperature Superconductors,* St. Andrews, 1991, edited by D. P. Tunstall and W. Barford, in High-T_c Superconductivity (Adam Hilger, New York, 1991), p. 169.
[96]B. Batlogg in *Electronic Properties of High-T_c Superconductors and Related* Compounds, edited by H. Kuzmany, M. Mehring, and J. Fink (Springer-Verlag, Berlin, 1990), p. 2.
[97]See, e.g., A. R. Moodenbaugh *et al.*, Phys. Rev B **38**, 4596 (1989); J. B. Torrance *et al.*, Phys. Rev. Lett. **61**, 1127 (1988); T. Takabatake *et al.*, Physica C **162-164**, 65 (1989); S. Tajima *et al. ibid.* **156**, 90 (1988); Y. J. Uemura *et al.*, Phys. Rev. Lett. **66**, 2665 (1991); L. Forro and J. R. Cooper, Europhys. Lett. **11**, 55 (1990), report a linear dependence of T_c with n_{3D} (calculated from the Hall number) for oxygen-deficient $Bi_2Sr_2CaCu_2O_{8-\delta}$, while also showing $\rho(0)$ increasing with increasing δ, indicative of nonoptimal superconductivity.
[98]J. J. Ladik, in *Organic Superconductivity,* edited by V. Z. Kresin and W. A. Little (Plenum, New York, 1990), p. 267.
[99]B. Bush and J. J. Lagowski, in *Organic Superconductivity,* edited by V. Z. Kresin and W. A. Little (Plenum, New York, 1990), p. 347.
[100]Using electrons having $m_{ab}^*=0.07m_e$ and assuming $\epsilon=11.5$ for the dielectric constant, we have $a_0^*=87$ Å. According to Eq. (10), the optimum quantum well spacing assuming $r_s^0=15$ would be $d=\sqrt{\pi}\beta_1 r_s^0 a_0^*=2300$ Å. According to Eq. (9) the electron density must be $n_{2D}=d^{-2}=1.9\times10^9$ cm^{-2}, the Fermi energy is $E_F^{2D}=65$ μeV, but by Eq. (11) the transition temperature is only $T_c\approx30$ mK. Using holes, on the other hand, and assuming $m_{ab}^*=0.48m_e$, we would have $a_0^*=13$ Å, $d\approx340$ Å, $n_{2D}=9\times10^{10}$ cm^{-2}, $E_F^{2D}=0.45$ meV, and $T_c=0.21$ K. Assuming $\epsilon=4.0\pm0.5$ for $YBa_2Cu_3O_7$ would imply $r_s^0=9$ and thus $d\approx200$ Å, $n_{2D}=2.5\times10^{11}$ cm^{-2}, $E_F^{2D}=1.25$ meV, and $T_c=0.58$ K. Of course, owing to possible mass renormalization and proximity effects, the superconducting parameters may not be the same as assumed above.